Vol. 604: 99–120, 2018
https://doi.org/10.3354/meps12742

MARINE ECOLOGY PROGRESS SERIES
Mar Ecol Prog Ser

Published October 4

Changes in zooplankton assemblages in northern Monterey Bay, California, during a fall transition

Julio B. J. Harvey[1,*], Jennifer L. Fisher[2], John P. Ryan[1], Shannon B. Johnson[1], William T. Peterson[3,‡], Robert C. Vrijenhoek[1]

[1]Monterey Bay Aquarium Research Institute, Moss Landing, California 95062, USA
[2]Cooperative Institute for Marine Resources Studies, Newport, Oregon 97365, USA
[3]National Oceanic and Atmospheric Administration, Northwest Fisheries Science Center, Seattle, Washington 98112, USA

ABSTRACT: Accurately assessing the diversity and abundance of marine zooplankton is greatly confounded by the interactions of biological and physical processes that vary in space and time. This study simultaneously assessed biological and physical sources of zooplankton assemblage variation with multidisciplinary methods. Autonomous underwater vehicles (AUVs) and shipboard plankton net sampling were used to document a seasonal shift that occurred during a typical fall transition period in northern Monterey Bay, California. Intrusion of low salinity offshore waters into our study region was associated with decreased stratification of the water column. Morphological taxonomy and high-throughput DNA sequencing (HTS), involving mitochondrial cytochrome oxidase subunit-I (COI) and large subunit (28S) nuclear ribosomal RNA, were used to document zooplankton communities in 36 vertical plankton tows collected during the fall transition. Increased copepod diversity and delivery of species associated with warmer southern waters corresponded with the intrusion of offshore waters. Echinoderms and barnacles also increased in abundance. Conversely, species of polychaetes and gastropods decreased in diversity and abundance. Onshore–offshore spatial shifts also occurred between August and October sampling periods. Primary insights contributed by newer methods included high resolution documentation of environmental variation (i.e. AUV data) and increased taxonomic resolution for some zooplankton groups (e.g. polychaetes and gastropods; HTS data) compared to the morphological assessment. Together, the AUV environmental data, morphological assessments and HTS zooplankton identifications provided a compelling picture of how water mass variation typical of the fall season can affect zooplankton assemblages in northern Monterey Bay, California.

KEY WORDS: Marine zooplankton · Biological oceanography · Plankton ecology · Upwelling shadow · Monterey Bay · California Current

INTRODUCTION

Seasonal upwelling of nutrient-rich deep water enhances primary productivity and supports diverse zooplankton communities in surface waters along the Central California margin (Ryther 1969, Barber & Smith 1981, Chavez & Messié 2009). Monterey Bay (see Fig. 1) lies within the eastern boundary upwelling ecosystem of the North Pacific (i.e. the California Current System). Wind-driven upwelling drives primary productivity that peaks during summer in this region, while fall is a time of transition to minimum upwelling during winter (Bakun 1973, Breaker & Broenkow 1994, Pennington & Chavez 2000). Relaxation of upwelling during the fall transition results in shoreward transport of offshore, low-salinity water from the California Current (Broenkow & Smethie 1978, Rosenfeld et al. 1994, Ramp et al. 2005). Further, the core of the California Current moves approximately 80 km closer to the coast dur-

*Corresponding author: jbjharvey@gmail.com
‡Deceased

ing fall (Collins et al. 2003). These seasonal shifts in physical oceanography deliver planktonic organisms and affect resident phytoplankton populations in Monterey Bay (Ryan et al. 2009, 2010b, 2014b). Spatial variation in zooplankton communities is also driven by the Monterey Bay upwelling shadow, a northern region of the bay protected from prevailing winds by coastal mountains and characterized by water mass recirculation and retention (Graham et al. 1992, Graham 1993). Northern Monterey Bay is relatively sheltered from strong atmospheric and oceanic circulation (Breaker & Broenkow 1994, Rosenfeld et al. 1994). This sheltering enhances vertical stratification and residence time in the northern bay and increases phytoplankton and zooplankton abundance (Graham & Largier 1997, Ryan et al. 2008, Woodson et al. 2009, Harvey et al. 2012). During fall, density stratification increases from a minimum at the mouth of Monterey Bay to a maximum at the northeastern areas of the upwelling shadow, and correspondingly affects plankton distributions (Ryan et al. 2008). These seasonal shifts coupled with the biological variability of zooplankton communities make it difficult to study the primary forces affecting diversity and abundance.

Autonomous underwater vehicles (AUVs) have provided environmental data at unparalleled spatial and temporal resolutions for an increasing number of oceanographic studies (Zhang et al. 2012, 2015, Ryan et al. 2014a,b, Harvey et al. 2017). Through synoptic characterization of physical and biological features (e.g. layers, convergent fronts, phytoplankton blooms), AUVs have enabled a better understanding of how physical and chemical variation in coastal environments affect planktonic organisms (Ryan et al. 2010a,b, 2014a,b). Monterey Bay Aquarium Research Institute's (MBARI's) 'Dorado' AUV has previously provided environmental data for zooplankton studies in Monterey Bay (Ryan et al. 2010a,b, 2014a, Harvey et al. 2012, Zhang et al. 2012). The 'Dorado' AUV is a valuable tool for assessing variation in environmental parameters (e.g. temperature, salinity, optical backscatter, nitrate, chlorophyll fluorescence) related to the spatial and temporal variation of zooplankton assemblages.

Zooplankton surveys typically rely on microscopy and morphological identifications of taxa, which are time-consuming and potentially biased by the taxonomic specializations and expertise of researchers (Harvey et al. 2017). Consequently, alternative methods for assessing zooplankton diversity have been explored, such as high-throughput DNA sequencing (HTS) (Caporaso et al. 2010, Lindeque et al. 2013, Hirai et al. 2015b, Bucklin et al. 2016). HTS offers advantages over morphological taxonomy, but significant methodological biases are well known, including problems with quantitative accuracy (Porazinska et al. 2009, Bik et al. 2012, Cowart et al. 2015, Harvey et al. 2017). Thus, HTS provides a welcome complement to, rather than a comprehensive replacement for morphological assessments (Hirai et al. 2015b, Harvey et al. 2017). Previous HTS-based assessments of zooplankton communities typically employed single genetic markers, e.g. the small subunit of the nuclear ribosomal RNA gene (18S rRNA) (Lindeque et al. 2013, Pearman et al. 2014, de Vargas et al. 2015, Hirai et al. 2015b), or the large subunit (28S) rRNA (Hirai et al. 2015a, Hirai & Tsuda 2015). The highly conserved nature of these genes typically limits taxonomic resolution to the family level, or above (Tang et al. 2012, Bucklin et al. 2016). The rapidly evolving mitochondrial cytochrome oxidase subunit-I (COI) gene can be used to assess genus- and species-level diversity in zooplankton communities (Machida et al. 2009, Bucklin et al. 2010, Cheng et al. 2014, Baek et al. 2016, Deagle et al. 2018), although COI primers typically amplify fewer species than ribosomal primers. COI-based HTS can identify potentially invasive propagules in ballast water (Zaiko et al. 2015), and accurately compare freshwater zooplankton communities (Yang et al. 2017).

We recently compared the effectiveness of traditional microscopy-based assessments with HTS surveys of COI and 28S for assessing zooplankton diversity in Monterey Bay, California (Harvey et al. 2017). HTS provided finer resolution of taxa for which morphological diagnostics were limited (e.g. polychaete larvae and fish eggs). However, HTS could not discriminate among life-stages of copepods and crab larvae that were distinguishable by microscopy. DNA sequence frequencies corresponded roughly with morphological assessments of biomass for some taxa, but significant correlations were gene-specific, and the results identified several methodological biases. Despite such biases, DNA-based alpha-diversity indices were concordant with morphology-based indices of zooplankton diversity across 4 sampling stations. However, the limited number of samples (n = 10) we initially analyzed precluded significant ecological inferences. In the present study, we extended these analyses to 36 samples collected during a period that spanned the fall transition. Samples collected during August and October 2013 were examined with HTS and morphological methods to assess the degree that shifts in regional oceanography influenced zooplankton assemblages in northern Monterey Bay.

MATERIALS AND METHODS

Environmental data

The MBARI M1 mooring and 'Dorado' AUV provided contextual environmental data during plankton sampling (www.mbari.org/products/data-repository/mooring-data/m1-mooring-summary-data/). Temperature and salinity were recorded hourly at the M1 mooring with a Sea-Bird Electronics CTD (Sea-Bird Scientific), located at the mouth of Monterey Bay, where the water depth is 1100 m (Fig. 1, black square). The 'Dorado' AUV conducted vertical profiles (0 to 80 m depths) of temperature and salinity (Sea-Bird Scientific) along transects connecting our sampling stations (Fig. 1, dashed line), during each day of sampling. AUV sections described environmental variation at finer spatial scales than ship CTD profiles in the northern Monterey Bay sampling area. Additionally, AUV surveys extending outside the bay identified the source of waters that moved into Monterey Bay during the 2013 fall transition. Monthly upwelling indices (36° N, 122° W) were taken from the National Oceanic and Atmospheric Administration's (NOAA) Environmental Research Division's Data Access Program (ERDDAP) server web portal (https://coastwatch.pfeg.noaa.gov/erddap/index.html).

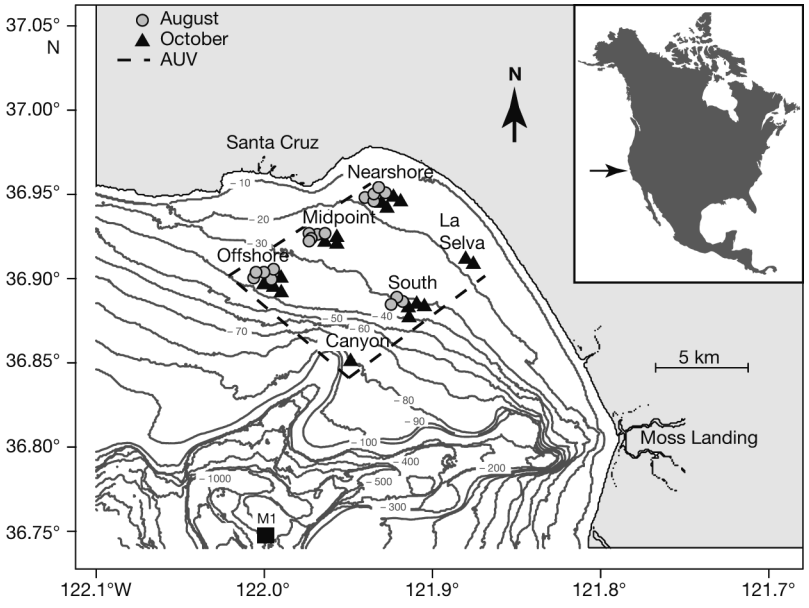

Fig. 1. Northern Monterey Bay, showing plankton net sample locations and sampling periods. Black square: location of mooring M1; dashed lines: concurrent AUV environmental survey transects. Sampling stations (Nearshore, Midpoint, Offshore, Canyon, South and La Selva) are labeled. Bathymetric lines appear at 10 m intervals to a depth of 100 m, and 100 m intervals thereafter

Sample collection and morphological data

As previously described (Harvey et al. 2017), 36 individual plankton samples were collected with a 0.75 m diameter, 200 µm mesh net during daylight hours from 12 to 16 August (n = 18) and from 22 to 25 October (n = 18) 2013, at stations in northern Monterey Bay (Fig. 1). Each sample consisted of 2 consecutive vertical net pulls (maximum net pull depth = 30 m; water depth range across sampling sites: 15 to 80 m). Cod-end contents were emptied onto a 170 µm mesh sieve and rinsed into sample containers. One subsample was preserved in buffered formalin (disodium tetraborate; 15 ml 37% solution 0.5 l^{-1} seawater) for morphological analysis and the second subsample was preserved in 80 to 90% ethanol for HTS analyses. As previously reported (Harvey et al. 2017), morphological subsamples were diluted and 1 to 10 ml aliquots were examined under a dissecting microscope to determine whether the density of zooplankton was small enough to process in 2 h. Samples that were too dense were split with a Folsom plankton splitter, and aliquots were counted as previously reported (Harvey et al. 2017). Zooplankton were identified with taxonomic keys (Fleminger 1967, Frost & Fleminger 1968, Lough 1974, Gardner & Szabo 1982, Shanks 2001). Counts of individuals were converted to biomass estimates (mg carbon m^{-3} seawater) using length–weight regressions, where carbon was assumed to be 40% of dry weight (Harvey et al. 2017), because biomass typically correlates better with HTS measures of abundance for zooplankton (Lindeque et al. 2013, Hirai et al. 2015a, Harvey et al. 2017).

Molecular analyses

Detailed methods for DNA isolation, target gene amplification, and HTS of sample libraries were previously reported (Harvey et al. 2017). Briefly, total DNA was isolated from ~30 µg of the cod-end contents from each plankton net sample (PowerSoil® DNA Isolation Kit; MO BIO Laboratories) and extraction products quantified with a NanoDrop™ 1000 spectrophotometer (Thermo Fisher Scientific). Previously published PCR primers (with M13 tags added) amplified portions of the mito-

chondrial COI (mlCOIintF/jgHCO2198; Geller et al. 2013, Leray et al. 2013) and the 28S nuclear ribosomal RNA (LSU26f/LSU657r; Park et al. 2015) with Ampitaq Gold® Fast PCR Master Mix (ThermoFisher Scientific) in triplicate, 25 µl reactions. A second round of PCR annealed 454 multiplex identifiers (Integrated DNA Technologies) to first round PCR products, to differentiate among samples after pooling and sequencing. After magnetic bead purification (Agencourt® AMPure® XP magnetic beads; Beckman Coulter), second round PCR products were quantified with a NanoDrop spectrophotometer, frozen, and sent to Macrogen (Seoul), where they were pooled and sequenced bi-directionally on 1/8th region of a 454 GSFLX Titanium plate.

Molecular data were processed with Quantitative Insights Into Microbial Ecology (QIIME) v.1.9.1 (Caporaso et al. 2010). As previously described in greater detail (Harvey et al. 2017), sequence data were demultiplexed, filtered and edited to remove primers and chimeric products (USEARCH v.6.1; Edgar 2010). Operational taxonomic unit (OTU) clusters with 97% similarity were created with UCLUST (Edgar 2010). While this level of clustering may condense highly similar species into a single OTU, we chose 97% to err on the side of caution with respect to overestimating species diversity. Taxonomic names were assigned to representative OTU sequences by comparing them to custom reference sequence databases with the Basic Local Alignment Search Tool (BLAST; Altschul et al. 1990), executed with QIIME (minimum percent identity = 95%, maximum e-value = 1.0^{-10}). A custom Python script, 'assign_taxonomy_blast_override.py' (Kyle Bittinger) was used to adjust minimum percent identity and maximum e-value with BLAST (https://groups.google.com/forum/#!topic/qiime-forum/kQO0JKcSE5w). Top scoring BLAST alignments were adopted as taxonomic identities. Custom reference sequence databases were created by downloading all eukaryotic COI and 28S sequences from the National Center for Biotechnology Information (NCBI; www.ncbi.nlm.nih.gov/nucleotide), and parsing them with 'gb2qiime.py' (McCann 2014), retaining only 1 identical replicate sequence taxon^{-1}. Molecular taxonomic assignments were verified by conducting independent BLAST searches with representative OTU sequences through NCBI's website (cut-off criteria for positive verification: query sequence coverage ≥75%, pairwise identity ≥95%). Where taxonomic ambiguity occurred, assignments were limited to the next highest taxonomic level. DNA sequence frequencies (percentage of total sequences in each sample library for each assigned taxon) were calculated to remove the effects of variation in the total number of next generation sequencing (NGS) sequences among sample libraries, similar to previous studies (Lindeque et al. 2013, Pearman et al. 2014, Hirai et al. 2015a, Harvey et al. 2017). For comparison of taxonomic levels above species, values for all lower taxa within each group (e.g. Genus) were combined. Taxonomic assignments and corresponding sequence frequencies were integrated into Biological Observation Matrix (BIOM) OTU tables. All HTS data were uploaded to NCBI (BioProjects PRJNA341398, PRJNA399732; BioSamples SAMN05721263–SAMN05721280, SAMN07549004–SAMN07549021; Sequence Read Archives SRP083968, SRP116118).

Statistical analysis

We assessed shifts in zooplankton diversity by estimating changes in species richness (the total number of species detected, averaged for each station within each sampling period, respectively) from the morphology (biomass estimates) and HTS data (COI and 28S OTU tables) sets. Data from the Canyon and La Selva stations (Fig. 1), sampled only in October, were excluded from multivariate analyses. Differences between sampling periods were tested with Student's *t*-tests, following Shapiro-Wilk tests (Royston 1982) to assess whether the data were normally distributed. All multivariate analyses were performed on Bray-Curtis dissimilarity matrices (Beals 1984, Faith et al. 1987) generated from arcsine-transformed HTS data. HTS DNA sequence frequencies were arcsine transformed to downweight abundant taxa and account for rare occurrences, after confirming that sample library sizes between the samples being compared were similar (i.e. ratio of largest to smallest mean sample library sizes were <1.5). Community-level changes were visualized with non-metric multidimensional scaling (NMDS; Minchin 1987) and tested for significance with a 2-way analysis of similarities (ANOSIM; Clarke 1993). ANOSIM tests for differences in the rank order of distance values between 2 or more groups of samples. The ANOSIM R-statistic varies in value from 0.0 to 1.0, with higher values indicating increasingly stronger rejection of the null hypothesis that there are no differences among groups (Clarke 1993). Analyses of M1 mooring and 'Dorado' AUV environmental data were conducted in MATLAB v.R2016b (MathWorks). A monthly 2013 upwelling index time series (NOAA ERDDAP) was overlain with salinity data from the M1 mooring. AUV temperature and

salinity values were quality-checked to remove aberrant data prior to generating point cloud and hydrographic curtain plots. Morphological and molecular data analyses were accomplished in R v.3.2.3 (R Core Team 2016) with RSTUDIO v.1.0.136 (RStudio Team 2016), primarily with the package 'phyloseq' (McMurdie & Holmes 2013). Additional required R packages were previously reported (Harvey et al. 2017). All R scripts are available in the Supplement at www.int-res.com/articles/suppl/m604p099_supp.txt.

RESULTS

Environmental context

Reduced upwelling and the intrusion of offshore waters into the northern Monterey Bay sampling area characterized the environmental shift between the 2 sampling periods. A seasonal decline in upwelling indices occurred between August and October (Fig. 2A). MBARI's M1 mooring (Fig. 1) recorded a concomitant decline in salinity that was consistent with the influx of low-salinity offshore water. Temperature and salinity recorded by the 'Dorado' AUV identified environmental differences between the August and October sampling periods (Fig. 2B). The August water column was more stratified with temperatures ranging from 10 to 16°C, whereas the October water column was more mixed with temperatures ranging from 11.5 to 14.5°C. Salinity was lower in October (Fig. 2B). AUV surveys conducted between the 2 sampling periods (Fig. 3A) show the influence of offshore low-salinity water entering this region of Monterey Bay (Fig. 3B). Lowest salinities occurring near the offshore end of Transect 1 originated from the California Current. The California Current water mixed with higher salinity water toward inner regions of the Bay (Transect 2, Fig. 3B) and extended into the surface waters at the northern portion of our sampling area. This transport and mixing of offshore, low-salinity water produced the shift in salinity observed between the August and October sampling periods (Fig. 2B).

Molecular data

Initial taxonomic assignment of the HTS data yielded a total of 74 710 COI sequences and 119 511 28S sequences. Only 10% of the total COI sequences and 2% of total 28S sequences were unassigned by the BLAST algorithm. Unassigned sequences (re-

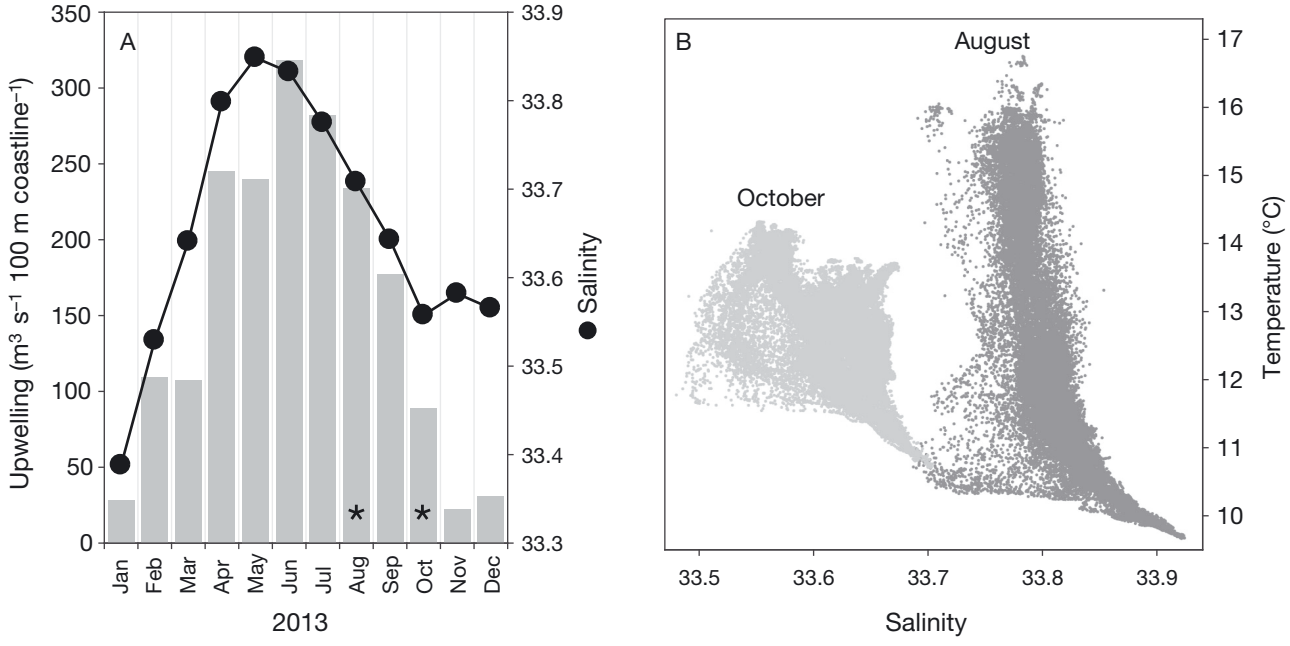

Fig. 2. Environmental data for northern Monterey Bay. (A) Monthly 2013 upwelling index time series (left-hand *y*-axis; NOAA's Environmental Research Division Data Access Program, ERDDAP) for 36° N, 122° W. Salinity data (right-hand *y*-axis; black dots: monthly mean, 10 m depth) collected at mooring M1 are overlaid. Asterisks indicate sampling months. (B) Autonomous underwater vehicle (AUV) temperature and salinity data for August (dark gray points) and October (light gray points) collected during plankton net sampling periods

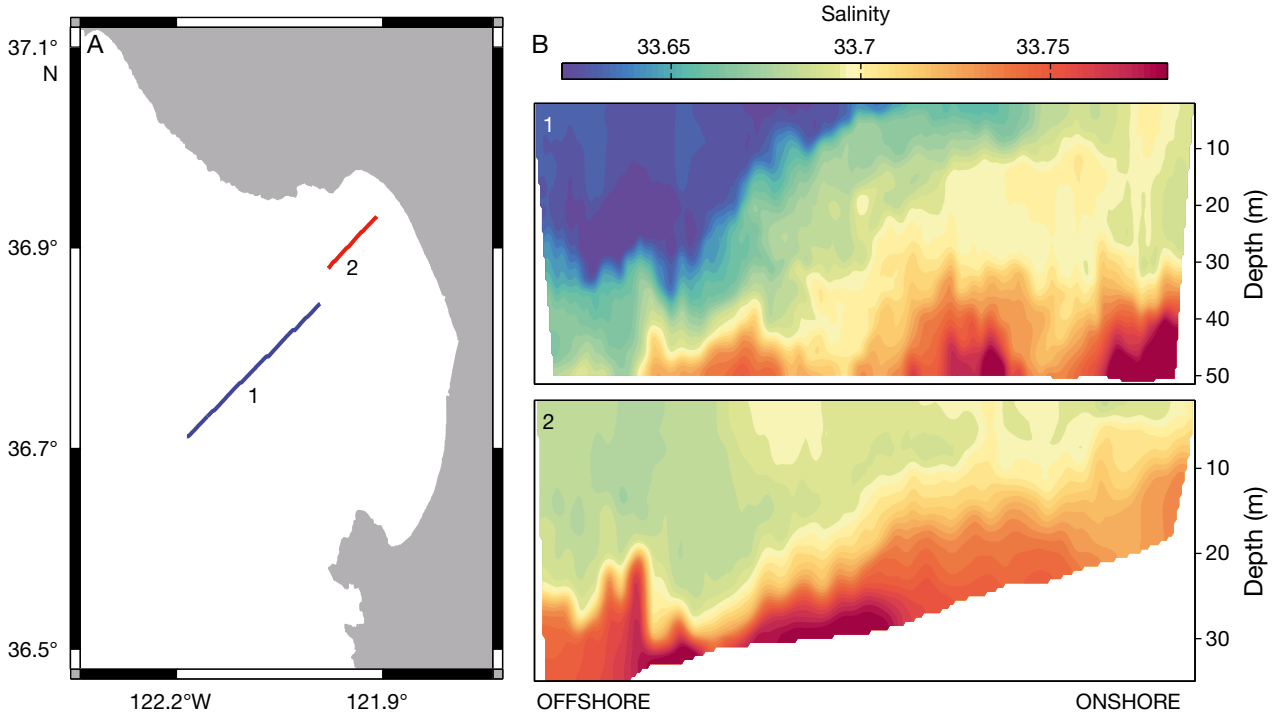

Fig. 3. Illustration of the source of low-salinity waters and their intrusion into Monterey Bay. (A) Locations of autonomous underwater vehicle (AUV) transects across the mouth of Monterey Bay (1; blue line) and in the northern bay plankton sampling area (2; red line). (B) Vertical sections of salinity for the AUV transects shown in (A). Numbers in the upper left-hand corners of each panel correspond to AUV surveys shown in (A). AUV surveys 1 and 2 were conducted between the fall 2013 plankton sampling periods, on 18 September and 1 October, respectively

moved from further analysis) corresponded to 16% of COI OTUs and 9% of 28S OTUs, respectively. One of the 36 samples (Stn Nearshore, August) had very small HTS library sizes (16 COI and 311 28S sequences); thus, we excluded this sample from further analysis (the original data can be obtained from the corresponding author). Of the 35 samples included in our analysis, an average of 2075 COI and 3319 28S sequences were generated per sample library. Maximum sample library sizes were 6172 (COI) and 9826 (28S). Minimum library sizes were 709 (COI) and 492 (28S). Altogether, COI identified 71 zooplankton genera, whereas 28S data identified 49 (Table 1). Because it provided finer taxonomic resolution, COI typically detected more taxa (i.e. to species level) than 28S. Custom reference sequence databases downloaded from NCBI were 6.47 gigabytes (COI) and 6.07 gigabytes (28S), respectively. After parsing, the COI database contained 194 450 taxa and the 28S database contained 187 464 taxa. Reference databases predominantly contained sequences corresponding to taxa detected by morphology, but there were exceptions (Table 1). In some cases, HTS data may not have identified taxa because no corresponding sequences for those taxa were present in the databases.

Richness and abundance

Morphological analysis of 14 samples identified 38 taxa to the finest taxonomic level possible. On average, biomass of the August samples was slightly greater (mean = 39.5 mg m^{-3} carbon, n = 10) than that of the October samples (mean = 34.4 mg m^{-3}, n = 3). The fourth October sample from the Nearshore station was not included because it contained only 9.6 mg m^{-3} carbon. Due to the limited number of samples analyzed morphologically, and to the conservative nature of taxonomic assignments based on 28S sequences (Harvey et al. 2017), the subsequent results focus primarily on analyses of the COI sequences, with support from 28S and morphology where possible.

The observed environmental shift was accompanied by changes in zooplankton species richness (Fig. 4) and biomass (Table 2) for some taxa. Mean richness was significantly higher in October for mor-

Table 1. Zooplankton taxa identified by high-throughput DNA sequencing (HTS ID) and morphology (M), and their occurrence in HTS databases

Phylum	Class	Order	Genus	Species	HTS ID		M	Database	
					COI	28S		COI	28S
Annelida	Polychaeta	—	—	sp.	+	+	+	+	+
Annelida	Polychaeta	Phascolosomatiformes	*Phascolosoma*	*agassizii*	+	+		+	+
Annelida	Polychaeta	Phyllodocida	*Aglaophamus*	*circinata*		+			+
Annelida	Polychaeta	Phyllodocida	*Bipalponephtys*	*cornuta*	+			+	+
Annelida	Polychaeta	Phyllodocida	*Halosydna*	*brevisetosa*	+			+	+
Annelida	Polychaeta	Phyllodocida	*Harmothoe*	*rarispina*	+			+	+
Annelida	Polychaeta	Phyllodocida	*Lepidasthenia*	*berkeleyae*	+			+	+
Annelida	Polychaeta	Phyllodocida	*Pholoides*	*asperus*	+			+	+
Annelida	Polychaeta	Sabellida	*Phragmatopoma*	*californica*	+			+	
Annelida	Polychaeta	Sabellida	*Sabellaria*	*cementarium*	+			+	
Annelida	Polychaeta	Spionida	*Phyllochaetopterus*	sp.		+		+	+
Annelida	Polychaeta	Spionida	*Prionospio*	*dubia*		+		+	+
Annelida	Polychaeta	Xenopneusta	*Urechis*	*caupo*	+			+	+
Arthropoda	Branchiopoda	Diplostraca	*Evadne*	*nordmanni*	+			+	+
Arthropoda	Branchiopoda	Diplostraca	*Evadne*	sp.	+		+	+	+
Arthropoda	Branchiopoda	Diplostraca	*Penilia*	*avirostris*	+			+	+
Arthropoda	Branchiopoda	Diplostraca	*Penilia*	sp.	+		+	+	+
Arthropoda	Branchiopoda	Diplostraca	*Podon*	sp.			+	+	+
Arthropoda	Malacostraca	Amphipoda	*Brachyscelus*	*rapax*		+		+	+
Arthropoda	Malacostraca	Decapoda	*Cancer*	*antennarius*	+			+	
Arthropoda	Malacostraca	Decapoda	*Cancer*	*gracilis*	+			+	+
Arthropoda	Malacostraca	Decapoda	*Cancer*	sp.	+		+	+	+
Arthropoda	Malacostraca	Decapoda	*Emerita*	*analoga*	+		+	+	+
Arthropoda	Malacostraca	Decapoda	*Emerita*	sp.	+	+		+	+
Arthropoda	Malacostraca	Decapoda	*Hemigrapsus*	sp.			+	+	+
Arthropoda	Malacostraca	Decapoda	*Lophopanopeus*	*bellus*	+			+	+
Arthropoda	Malacostraca	Decapoda	*Lophopanopeus*	sp.	+		+	+	+
Arthropoda	Malacostraca	Decapoda	*Majidae*	sp.			+	+	+
Arthropoda	Malacostraca	Decapoda	*Mimulus*	*foliatus*	+			+	+
Arthropoda	Malacostraca	Decapoda	*Neotrypaea*	*californiensis*		+		+	
Arthropoda	Malacostraca	Decapoda	*Pachycheles*	sp.			+	+	+
Arthropoda	Malacostraca	Decapoda	*Pachygrapsus*	sp.			+	+	+
Arthropoda	Malacostraca	Decapoda	*Paguridae*	sp.			+	+	+
Arthropoda	Malacostraca	Decapoda	*Paguristes*	sp.			+		+
Arthropoda	Malacostraca	Decapoda	*Pinnixa*	*faba*	+	+		+	+
Arthropoda	Malacostraca	Decapoda	*Pinnotheridae*	sp.	+	+	+	+	+
Arthropoda	Malacostraca	Decapoda	*Pugettia*	*richii*	+			+	+
Arthropoda	Malacostraca	Decapoda	*Pugettia*	sp.	+		+	+	+
Arthropoda	Malacostraca	Euphausiacea	—	sp.	+	+	+	+	+
Arthropoda	Malacostraca	Euphausiacea	*Euphausia*	*pacifica*	+		+	+	+
Arthropoda	Malacostraca	Euphausiacea	*Euphausia*	sp.	+	+	+	+	+
Arthropoda	Malacostraca	Euphausiacea	*Nematoscelis*	*difficilis*	+			+	
Arthropoda	Malacostraca	Euphausiacea	*Nematoscelis*	sp.	+	+		+	+
Arthropoda	Malacostraca	Euphausiacea	*Thysanoessa*	*spinifera*	+		+	+	+
Arthropoda	Maxillopoda	(Copepoda)	—	sp.	+	+	+	+	+
Arthropoda	Maxillopoda	Calanoida	*Acartia*	*californiensis*	+			+	
Arthropoda	Maxillopoda	Calanoida	*Acartia*	*hudsonica*			+	+	
Arthropoda	Maxillopoda	Calanoida	*Acartia*	*longiremis*			+	+	+
Arthropoda	Maxillopoda	Calanoida	*Acartia*	sp.	+			+	+
Arthropoda	Maxillopoda	Calanoida	*Acartia*	*tonsa*			+	+	+
Arthropoda	Maxillopoda	Calanoida	*Bathycalanus*	sp.		+		+	+
Arthropoda	Maxillopoda	Calanoida	*Calanus*	*marshallae*			+	+	+
Arthropoda	Maxillopoda	Calanoida	*Calanus*	*pacificus*	+		+	+	+
Arthropoda	Maxillopoda	Calanoida	*Calanus*	*sinicus*		+		+	+
Arthropoda	Maxillopoda	Calanoida	*Calanus*	sp.	+	+	+	+	+
Arthropoda	Maxillopoda	Calanoida	*Calocalanus*	*pavo*			+	+	+
Arthropoda	Maxillopoda	Calanoida	*Calocalanus*	*styliremis*			+		+
Arthropoda	Maxillopoda	Calanoida	*Calocalanus*	*tenuis*	+		+	+	
Arthropoda	Maxillopoda	Calanoida	*Candacia*	*bipinnata*	+			+	+
Arthropoda	Maxillopoda	Calanoida	*Clausocalanus*	*arcuicornis*			+	+	+
Arthropoda	Maxillopoda	Calanoida	*Clausocalanus*	*furcatus*	+		+	+	+

Table 1 (continued)

Phylum	Class	Order	Genus	Species	HTS ID		M	Database	
					COI	28S		COI	28S
Arthropoda	Maxillopoda	Calanoida	*Clausocalanus*	*jobei*	+			+	
Arthropoda	Maxillopoda	Calanoida	*Clausocalanus*	*lividus*		+		+	+
Arthropoda	Maxillopoda	Calanoida	*Clausocalanus*	*parapergens*	+			+	+
Arthropoda	Maxillopoda	Calanoida	*Clausocalanus*	*pergens*	+		+	+	+
Arthropoda	Maxillopoda	Calanoida	*Clausocalanus*	sp.	+	+	+	+	+
Arthropoda	Maxillopoda	Calanoida	*Cosmocalanus*	*darwinii*	+	+		+	+
Arthropoda	Maxillopoda	Calanoida	*Ctenocalanus*	*vanus*	+	+	+	+	+
Arthropoda	Maxillopoda	Calanoida	*Epilabidocera*	*amphitrites*			+		
Arthropoda	Maxillopoda	Calanoida	*Eucalanus*	*californicus*	+	+			+
Arthropoda	Maxillopoda	Calanoida	*Eucalanus*	sp.	+	+	+	+	+
Arthropoda	Maxillopoda	Calanoida	*Eucalanus*	*subtenuis*	+			+	+
Arthropoda	Maxillopoda	Calanoida	*Labidocera*	*scotti*		+			+
Arthropoda	Maxillopoda	Calanoida	*Metridia*	*brevicauda*		+			+
Arthropoda	Maxillopoda	Calanoida	*Metridia*	*lucens*	+			+	+
Arthropoda	Maxillopoda	Calanoida	*Metridia*	*pacifica*		+		+	+
Arthropoda	Maxillopoda	Calanoida	*Metridia*	sp.	+	+	+	+	+
Arthropoda	Maxillopoda	Calanoida	*Microcalanus*	*pusillus*			+		
Arthropoda	Maxillopoda	Calanoida	*Paracalanus*	*aculeatus*		+		+	+
Arthropoda	Maxillopoda	Calanoida	*Paracalanus*	*parvus*			+	+	+
Arthropoda	Maxillopoda	Calanoida	*Paracalanus*	sp.	+	+	+	+	+
Arthropoda	Maxillopoda	Calanoida	*Pleuromamma*	*gracilis*		+		+	+
Arthropoda	Maxillopoda	Calanoida	*Pseudocalanus*	*mimus*	+	+		+	+
Arthropoda	Maxillopoda	Calanoida	*Pseudocalanus*	*minutus*		+		+	+
Arthropoda	Maxillopoda	Calanoida	*Pseudocalanus*	*newmani*	+			+	
Arthropoda	Maxillopoda	Calanoida	*Pseudocalanus*	sp.	+	+	+	+	+
Arthropoda	Maxillopoda	Calanoida	*Rhincalanus*	*nasutus*	+	+	+	+	+
Arthropoda	Maxillopoda	Calanoida	*Temora*	*discaudata*	+			+	+
Arthropoda	Maxillopoda	Calanoida	*Tortanus*	*discaudatus*			+	+	
Arthropoda	Maxillopoda	Cyclopoida	*Oithona*	*similis*		+	+	+	+
Arthropoda	Maxillopoda	Cyclopoida	*Oithona*	*spinirostris*			+		
Arthropoda	Maxillopoda	Pedunculata	*Pollicipes*	*caboverdensis*	+			+	
Arthropoda	Maxillopoda	Pedunculata	*Pollicipes*	*polymerus*	+		+	+	+
Arthropoda	Maxillopoda	Poecilostomatoida	*Corycaeus*	*anglicus*			+	+	+
Arthropoda	Maxillopoda	Poecilostomatoida	*Oncaea*	*media*		+			+
Arthropoda	Maxillopoda	Poecilostomatoida	*Oncaea*	*scottodicarloi*	+			+	
Arthropoda	Maxillopoda	Poecilostomatoida	*Oncaea*	sp.	+	+	+	+	+
Arthropoda	Maxillopoda	Sessilia	*Balanidae*	sp.	+	+	+	+	+
Arthropoda	Maxillopoda	Sessilia	*Balanus*	*balanus*	+			+	+
Arthropoda	Maxillopoda	Sessilia	*Balanus*	*crenatus*			+	+	+
Arthropoda	Maxillopoda	Sessilia	*Balanus*	*glandula*		+	+	+	+
Arthropoda	Maxillopoda	Sessilia	*Balanus*	*nubilus*			+		
Arthropoda	Maxillopoda	Sessilia	*Balanus*	*trigonus*	+			+	+
Arthropoda	Maxillopoda	Sessilia	*Chthamalus*	*dalli*	+			+	
Arthropoda	Maxillopoda	Sessilia	*Chthamalus*	*fissus*	+			+	
Arthropoda	Maxillopoda	Sessilia	*Chthamalus*	sp.	+		+	+	+
Arthropoda	Maxillopoda	Sessilia	*Notochthamalus*	*scabrosus*		+		+	+
Arthropoda	Maxillopoda	Sessilia	*Tetraclita*	*rubescens*	+			+	
Arthropoda	Ostracoda	—	—	sp.			+	+	+
Arthropoda	Ostracoda	Halocyprida	*Discoconchoecia*	*elegans*	+			+	
Brachiopoda	Lingulata	Lingulida	*Glottidia*	*pyramidata*		+			+
Bryozoa	—	—	—	sp.			+	+	+
Bryozoa	Gymnolaemata	Cheilostomatida	*Membranipora*	*serrilamella*	+			+	
Chaetognatha	—	—	—	sp.			+	+	+
Chordata	Actinopteri	—	—	sp.	+		+	+	
Chordata	Actinopteri	NA	*Genyonemus*	*lineatus*	+			+	
Chordata	Actinopteri	Pleuronectiformes	*Citharichthys*	*sordidus*	+			+	
Chordata	Actinopteri	Pleuronectiformes	*Citharichthys*	*stigmaeus*	+			+	
Chordata	Actinopteri	Pleuronectiformes	*Paralichthys*	*californicus*	+			+	+
Chordata	Actinopteri	Pleuronectiformes	*Psettichthys*	*melanostictus*	+			+	
Chordata	Appendicularia	—	*Oikopleura*	sp.			+		+
Chordata	Thaliacea	Doliolida	*Dolioletta*	*gegenbauri*			+		
Cnidaria	Hydrozoa	Leptothecata	*Laomedea*	*angulata*		+			+

Table 1 (continued)

Phylum	Class	Order	Genus	Species	HTS ID		M	Database	
					COI	28S		COI	28S
Cnidaria	Hydrozoa	Siphonophorae	*Erenna*	*insidiator*		+			+
Cnidaria	Hydrozoa	Siphonophorae	*Lensia*	*campanella*	+			+	
Cnidaria	Hydrozoa	Siphonophorae	*Lensia*	*conoidea*		+		+	+
Cnidaria	Hydrozoa	Siphonophorae	*Muggiaea*	*atlantica*		+			+
Cnidaria	Hydrozoa	Siphonophorae	*Muggiaea*	sp.		+	+		+
Cnidaria	Hydrozoa	Siphonophorae	*Nectopyramis*	sp.		+		+	+
Cnidaria	Hydrozoa	Siphonophorae	*Sphaeronectes*	*gracilis*	+			+	
Cnidaria	Hydrozoa	Trachymedusae	*Geryonia*	*proboscidalis*	+		+	+	
Cnidaria	Scyphozoa	Semaeostomeae	*Chrysaora*	*fuscescens*		+			+
Ctenophora	Nuda	Beroida	*Beroe*	*ovata*		+			+
Ctenophora	Tentaculata	Cydippida	*Pleurobrachia*	sp.			+		+
Echinodermata	—	—	—	sp.	+	+	+	+	+
Echinodermata	Asteroidea	Forcipulatida	*Pisaster*	*brevispinus*	+			+	+
Echinodermata	Asteroidea	Forcipulatida	*Pisaster*	*giganteus*	+			+	+
Echinodermata	Asteroidea	Forcipulatida	*Rathbunaster*	*californicus*	+			+	+
Echinodermata	Asteroidea	Paxillosida	*Luidia*	*foliolata*	+			+	+
Echinodermata	Echinoidea	Cassiduloida	*Echinolampas*	*crassa*		+			+
Echinodermata	Echinoidea	Clypeasteroida	*Dendraster*	*excentricus*	+			+	
Echinodermata	Ophiuroidea	Ophiurida	*Amphiodia*	*urtica*	+			+	
Echinodermata	Ophiuroidea	Ophiurida	*Amphipholis*	sp.	+			+	+
Echinodermata	Ophiuroidea	Ophiurida	*Ophiopholis*	*aculeata*	+			+	+
Echinodermata	Ophiuroidea	Ophiurida	*Ophiopholis*	*kennerlyi*	+			+	
Echinodermata	Ophiuroidea	Ophiurida	*Ophiopholis*	*longispina*	+			+	
Echinodermata	Ophiuroidea	Ophiurida	*Ophiopholis*	sp.	+			+	+
Echinodermata	Ophiuroidea	Ophiurida	*Ophiophragmus*	*filograneus*		+			+
Echinodermata	Ophiuroidea	Ophiurida	*Ophiopteris*	*papillosa*	+			+	+
Echinodermata	Ophiuroidea	Ophiurida	*Ophiothrix*	*angulata*		+		+	+
Mollusca	Bivalvia	—	—	sp.	+	+	+	+	+
Mollusca	Bivalvia	Myoida	*Hiatella*	*arctica*		+			+
Mollusca	Bivalvia	Mytiloida	*Modiolus*	*modiolus*		+		+	+
Mollusca	Bivalvia	Mytiloida	*Modiolus*	sp.		+		+	+
Mollusca	Bivalvia	Mytiloida	*Mytilus*	*edulis*		+		+	+
Mollusca	Bivalvia	Veneroida	*Mysella*	*charcoti*		+			+
Mollusca	Bivalvia	Veneroida	*Pseudopythina*	*ariake*		+			+
Mollusca	Bivalvia	Veneroida	*Serripes*	sp.		+		+	+
Mollusca	Bivalvia	Veneroida	*Vesicomya*	*stearnsii*	+			+	
Mollusca	Gastropoda	—	—	sp.	+	+	+	+	+
Mollusca	Gastropoda	—	*Aglaja*	*ocelligera*	+			+	
Mollusca	Gastropoda	—	*Amphissa*	*columbiana*		+		+	+
Mollusca	Gastropoda	—	*Amphissa*	*reticulata*	+			+	
Mollusca	Gastropoda	—	*Crepipatella*	*lingulata*	+			+	+
Mollusca	Gastropoda	—	*Lacuna*	*vincta*	+			+	+
Mollusca	Gastropoda	—	*Mitrella*	*tuberosa*	+			+	
Mollusca	Gastropoda	—	*Nassarius*	*mendicus*	+	+		+	+
Mollusca	Gastropoda	—	*Olivella*	*baetica*	+			+	
Mollusca	Gastropoda	—	*Olivella*	*biplicata*	+			+	+
Mollusca	Gastropoda	—	*Rictaxis*	*punctocaelatus*	+			+	+
Mollusca	Gastropoda	Nudibranchia	*Acanthodoris*	*lutea*	+			+	
Mollusca	Gastropoda	Nudibranchia	*Aeolidia*	sp.	+			+	+
Mollusca	Gastropoda	Nudibranchia	*Goniodoris*	*nodosa*		+			+
Mollusca	Gastropoda	Nudibranchia	*Hermissenda*	*opalescens*	+			+	
Mollusca	Gastropoda	Nudibranchia	*Melibe*	*leonina*	+			+	
Mollusca	Gastropoda	Nudibranchia	*Onchidoris*	*bilamellata*	+			+	+
Mollusca	Gastropoda	Nudibranchia	*Triopha*	*catalinae*	+			+	+
Mollusca	Gastropoda	Nudibranchia	*Tritonia*	*diomedea*	+			+	
Mollusca	Gastropoda	Nudibranchia	*Tritonia*	*festiva*	+			+	
Mollusca	Gastropoda	Thecosomata	*Corolla*	*spectabilis*	+			+	
Mollusca	Gastropoda	Thecosomata	*Limacina*	sp.			+	+	+
Nemertea	—	—	—	sp.			+	+	+
Nemertea	Anopla	Heteronemertea	*Lineus*	*alborostratus*		+			+
Nemertea	Anopla	Heteronemertea	*Maculaura*	sp.		+		+	+
Radiolaria	—	—	—	sp.			+		

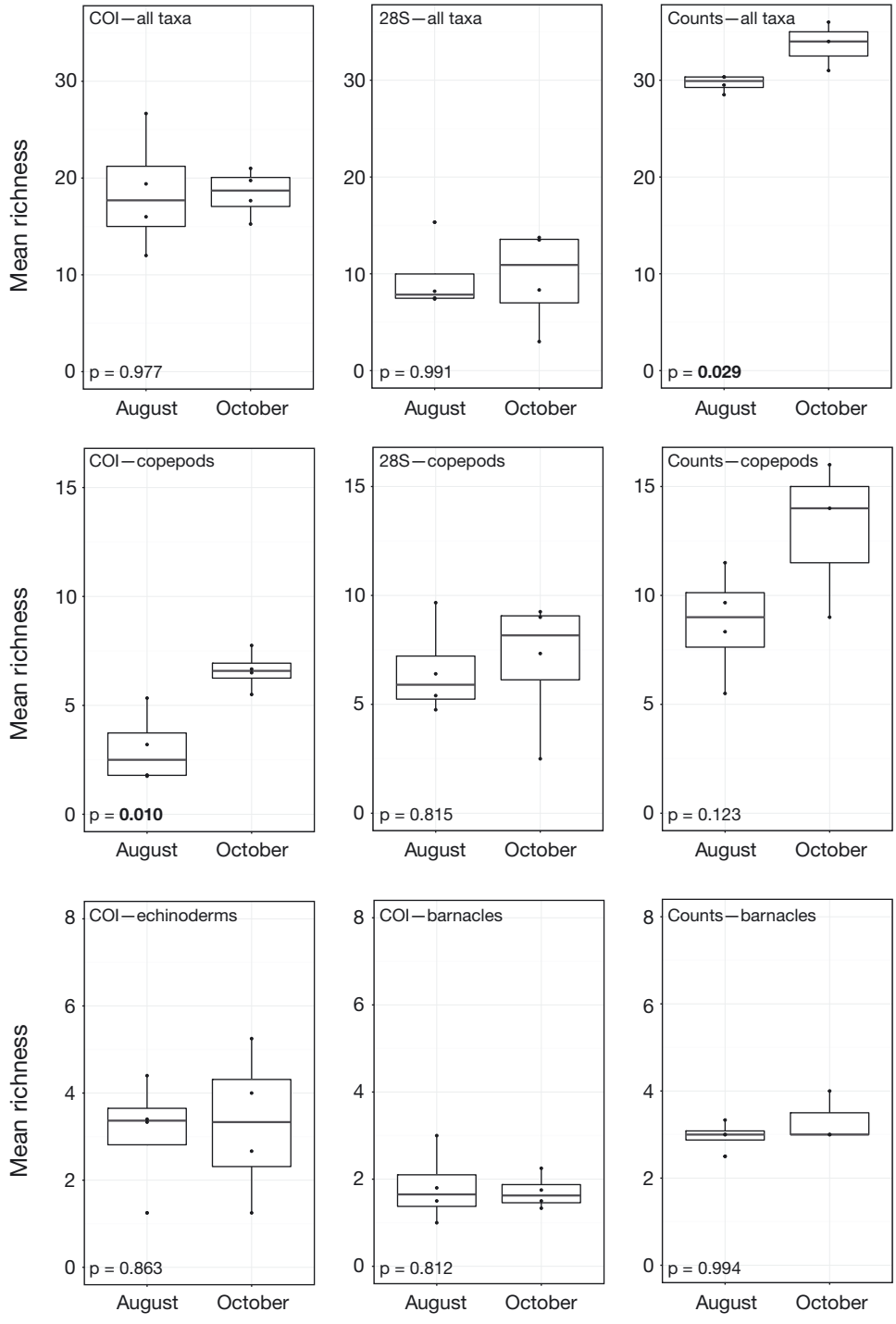

Fig. 4. Zooplankton richness (averaged for each station) in August and October for all taxa detected, copepods, echinoderms and barnacles. Data sets corresponding to each plot are indicated (upper left-hand corners). Student's *t*-test results are indicated in lower left-hand corners. Significant values ($p < 0.05$) are in **bold**. For high-throughput DNA sequencing (HTS) data (COI and 28S), only stations sampled during both periods were included (i.e. Nearshore, Midpoint, Offshore, and South). For biomass data, the Canyon station was also included. Non-parametric boxplots overlay data points; bold middle line: median, 50% quartile; lower and upper box hinges: 25% (Q1) and 75% (Q3) quartiles respectively; lower whisker: smallest observation ≥ lower hinge value − 1.5 × interquartile range (IQR = Q3 − Q1); upper whisker: largest observation ≤ upper hinge value + 1.5 × IQR. Richness data were averaged across samples collected at each station. Some data sets were not included due to their lack of variation between sampling periods (e.g. echinoderm and barnacle 28S)

Table 2. Mean zooplankton biomass for August and October sampling periods. **Bold:** major taxonomic groups

	Biomass (mg C m^{-3} seawater) August	October
Copepoda	25.880	21.561
Acartia	15.511	9.195
Calanus	0.734	2.720
Calocalanus	0.016	0.059
Clausocalanus	0.012	3.501
Corycaeus	0.360	0.402
Ctenocalanus	0.482	1.219
Epilabidocera	0.173	0.322
Eucalanus	0.120	0.206
Metridia	0.204	0.000
Microcalanus	0.000	0.003
Oithona	1.806	0.235
Oncaea	0.001	0.002
Paracalanus	4.961	2.102
Pseudocalanus	0.661	0.363
Rhincalanus	0.000	0.474
Tortanus	0.837	0.754
Echinodermata	0.079	0.170
Sessilia	0.057	0.243
Balanus	0.050	0.226
Cthamalus	0.007	0.017
Polychaeta	0.295	0.246
Gastropoda	0.059	0.014
Decapoda	1.606	2.823
Cancer	0.428	0.573
Emerita	0.695	0.302
Hemigrapsus	0.183	0.000
Lophopanopeus	0.121	0.000
Majidae	0.007	0.000
Pachycheles	0.015	0.000
Pachygrapsus	0.003	0.000
Paguridae	0.030	0.000
Paguristes	0.089	0.094
Pinnotheridae	0.029	1.853
Pugettia	0.006	0.000
Actinopteri	0.030	0.429
Euphausiacea	1.366	0.030
Euphausia	1.049	0.030
Thysanoessa	0.317	0.000

phological counts of all zooplankton taxa ($p = 0.029$) and for copepod COI sequences ($p = 0.010$). COI sequence frequencies revealed changes in copepod diversity (Fig. 5A,D). For example, *Calocalanus tenuis*, *Cosmocalanus darwinii*, *Rhincalanus nasutus* and *Temora discaudata* sequences were only found during October, whereas *Metridia lucens* sequences were only found in August. *Acartia californiensis*, *Calanus pacificus*, *Clausocalanus* (*C. furcatus*, *C. jobei*, *C. parapergens*, *C. pergens*), and *Paracalanus* sequence frequencies increased between the sampling periods. These increases in COI sequence frequencies corresponded with increases in mean copepod biomass for some taxa (e.g. *Calanus*; Table 2) but not others (e.g. *Acartia*). Overall, mean copepod biomass decreased slightly between sampling periods.

Mean echinoderm biomass increased between August and October (Table 2), but taxa within the phylum were not differentiated morphologically. Although echinoderm COI richness did not differ (Fig. 4), the frequencies of various sequences changed between sampling periods (Fig. 5B,E). *Dendraster excentricus* (sand dollar) sequences were abundant during both periods, but their relative frequency was greater in August (Fig. 5B). Conversely, sequences for 2 ophiuroid species (*Ophiopteris papillosa* and *Amphiodia urtica*) were more frequent in October. *Rathbunaster californicus* sequences were only detected during October (Fig. 5E).

Barnacle richness also remained stable between sampling periods (Fig. 4), but again, sequence frequencies shifted for some taxa. *Balanus* (*B. balanus*, *B. trigonus*), *Chthamalus* (*C. dalli*, *C. fissus*) and *Pollicipes* (*P. caboverdensis*, *P. polymerus*) sequences were detected during both periods, whereas *Tetraclita rubescens* was only detected in October (Fig. 5C,F). An increase in the frequency of *Balanus* sequences corresponded with an increase in biomass for that genus (Table 2).

Species richness was lower in October for several taxa. Mean COI richness was lower for polychaetes and gastropods, and the mean richness of morphological counts was reduced for crabs in October (Fig. 6). Only the gastropod decrease was significant ($p = 0.029$). More polychaete and gastropod genera were detected during August (Fig. 7A,B). The polychaetes *Phragmatopoma californica* and *Halosydna brevisetosa*, and the gastropods *Crepipatella lingulata*, *Hermissenda opalescens*, *Mitrella tuberosa*, and *Olivella* (*O. baetica*, *O. biplicata*) were observed during both sampling periods. These reductions in richness and COI sequence frequencies corresponded with decreases in mean biomass of polychaetes and gastropods (Table 2). Except for *Pugettia*, COI sequences from most crab genera were detected during both sampling periods (Fig. 7C,F). Although mean crab biomass increased between sampling periods (Table 2), sequence frequencies for various crab genera remained similar.

Community variation

Seasonal shifts in community composition were revealed with NMDS ordinations of Bray-Curtis distances estimated from the DNA sequence data (Fig. 8). The HTS data identified statistically sig-

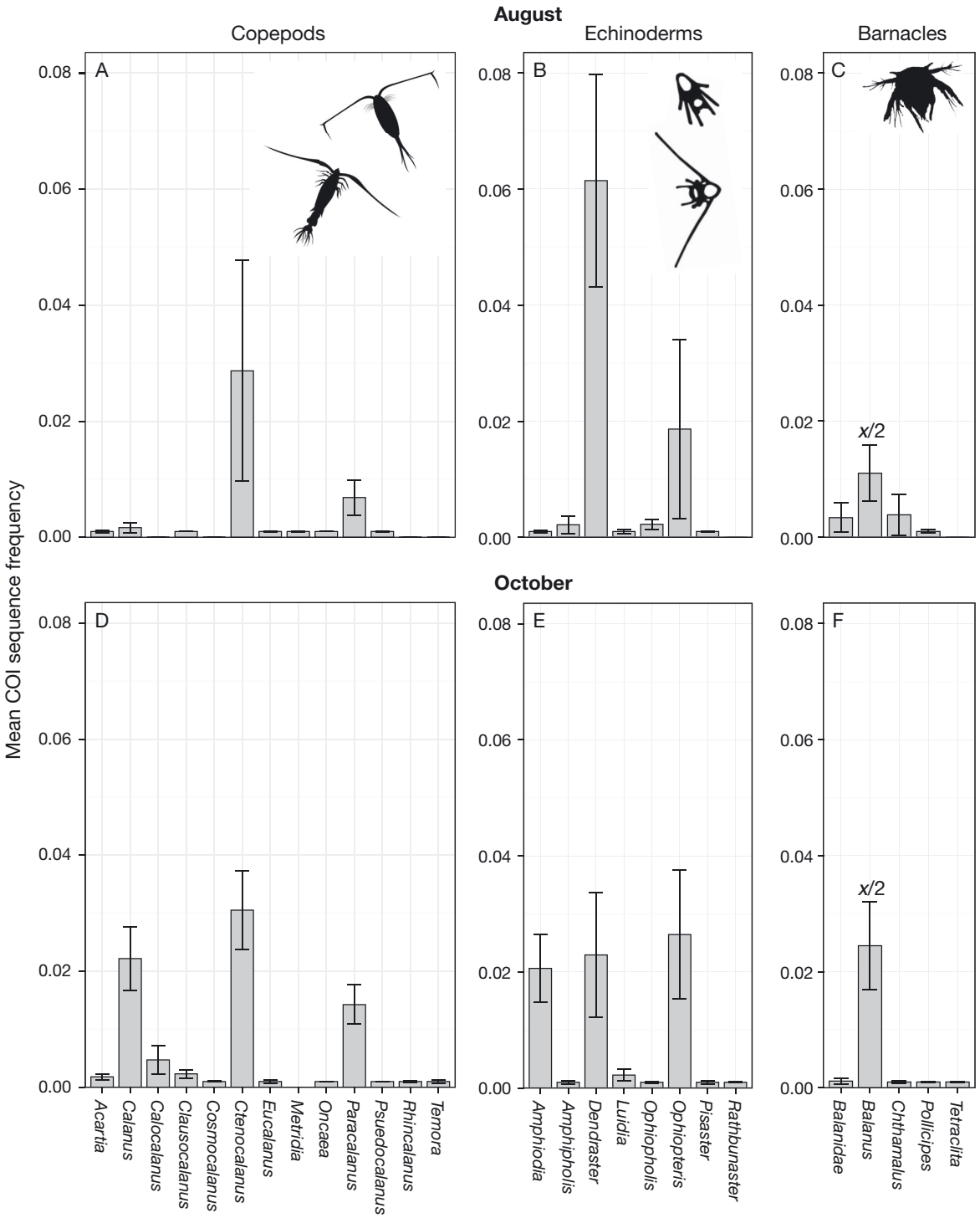

Fig. 5. Variation in mean COI sequence frequencies for (A,D) copepods, (B,E) echinoderms and (C,F) barnacles between August (A–C) and October (D–F) sampling periods. Mean COI sequence frequencies (*y*-axes; % total sample library size) are shown for various genera (*x*-axes). For *Balanus*, *x*/2 indicates scaling of *y*-axis values by one-half to facilitate visualization; *y*-axis values >0 but <0.001 were plotted as 0.001 improve presence/absence visualization. Error bars: SE

nificant shifts for all taxa and for copepods, echinoderms and polychaetes (ANOSIM, $p < 0.01$). Significant differences also existed among sampling stations for all taxa and for copepods and polychaetes (ANOSIM, $p < 0.01$; in the Appendix). The COI data revealed stronger seasonal shifts for all taxa and copepods (i.e. higher ANOSIM R-values) than the 28S data. Significant shifts were not

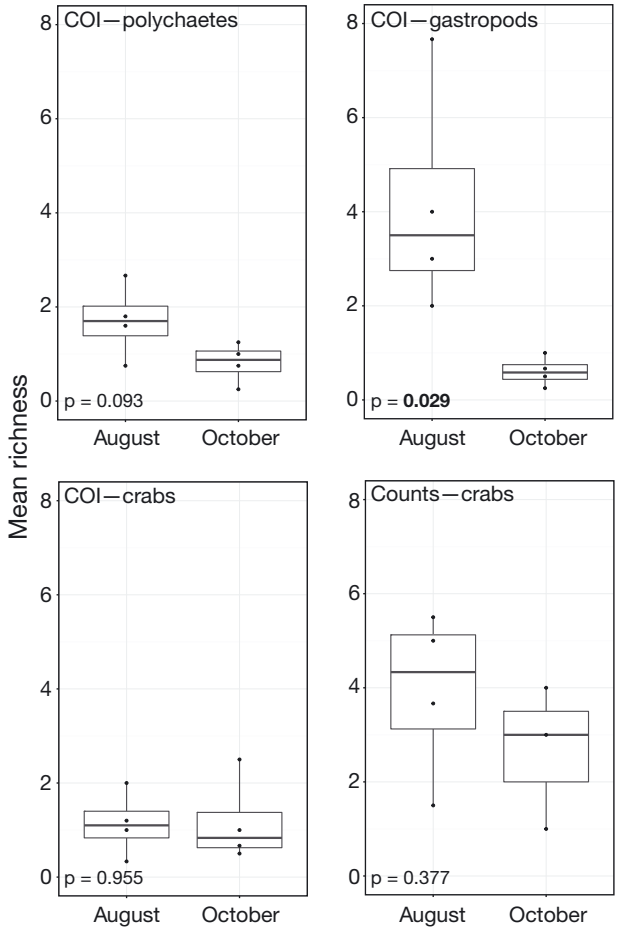

Fig. 6. Zooplankton richness (averaged for each station) in August and October for polychaetes, gastropods and crabs. Data sets corresponding to each plot are indicated (upper left-hand corners). Student's *t*-test results are indicated in lower left-hand corners. Significant values ($p < 0.05$) are in **bold**. For high-throughput DNA sequencing (HTS) data (COI and 28S), only stations sampled during both periods were included (i.e. Nearshore, Midpoint, Offshore, and South). For biomass data, the Canyon station was also included. Non-parametric boxplots overlay data points; bold middle line: median, 50% quartile; lower and upper box hinges: 25% (Q1) and 75% (Q3) quartiles respectively; lower whisker: smallest observation ≥ lower hinge value − 1.5 × interquartile range (IQR = Q3 − Q1); upper whisker: largest observation ≤ upper hinge value + 1.5 × IQR. Richness data were averaged across samples collected at each station. Some data sets were not included due to their lack of variation between sampling periods (e.g. 28S data)

observed for barnacles or crabs. For echinoderms, polychaetes, barnacles and crabs, 28S data were too sparse for ordination. Because the morphological data were generated for a smaller subset of samples (August, n = 10; October, n = 3), ordination of distances was uninformative.

Spatial changes in abundance

Seasonal shifts in the frequencies and biomass of various taxa also occurred among sampling stations examined in this study (Fig. 9), although this was not the case for all taxa (e.g. copepods). For example, frequencies of COI sequences for *Dendraster* were greatest at the Offshore and Midpoint stations during August, and greatest at the Canyon station during October. Similarly, *Ophiopteris* sequences were most frequent at the Nearshore station during August and the Canyon station during October. *Amphiodia* sequences were barely detected during August, but they increased at all stations during October. Similar to some echinoderm COI frequencies, echinoderm biomass was greatest at the furthest stations from shore (Stn Offshore in August and Stn Canyon in October; Table 3). Results for 28S were uninformative with respect to spatial distributions of organisms.

The COI frequencies of other taxa also shifted among stations between sampling periods (Fig. 9). For example, polychaete sequence frequencies were greatest at the Offshore and Midpoint stations during August and reduced there in October. Peaks in polychaete COI frequencies at the Midpoint station in August and the Canyon station in October corresponded with polychaete biomass maxima (Table 3). Conversely, crab biomass fluctuations did not appear to correspond with variations in COI sequence frequencies among stations. Nevertheless, presence/absence detection of crab COI sequences indicated a distributional shift between sampling periods; with the exception of *Cancer*, crabs occurred at all stations during August but at only 2 stations during October (Fig. 9). COI data also suggested distributional shifts for fish. *Genyonemus* (white croaker) was only detected at the Offshore site in August but occurred at all stations except Canyon in October. Conversely, flatfish (e.g. the sanddab *Citharichthys*) were identified by COI at all stations in August but were only present at the Canyon and La Selva stations in October.

Unlike other taxa, *Euphausia pacifica* COI sequences were detected at every station during both sampling periods, but spatial differences existed. *E. pacifica* COI frequencies and biomass were greatest at stations furthest from shore (i.e. Stns Offshore and South), and decreased shoreward during August (Fig. 9, Table 3). Similarly, *Thysanoessa spinifera* COI frequencies were greatest at the Offshore and South stations in August, however, *T. spinifera* biomass values were not concordant with sequence frequencies. Overall, euphausiid biomass decreased between sampling periods (Table 2).

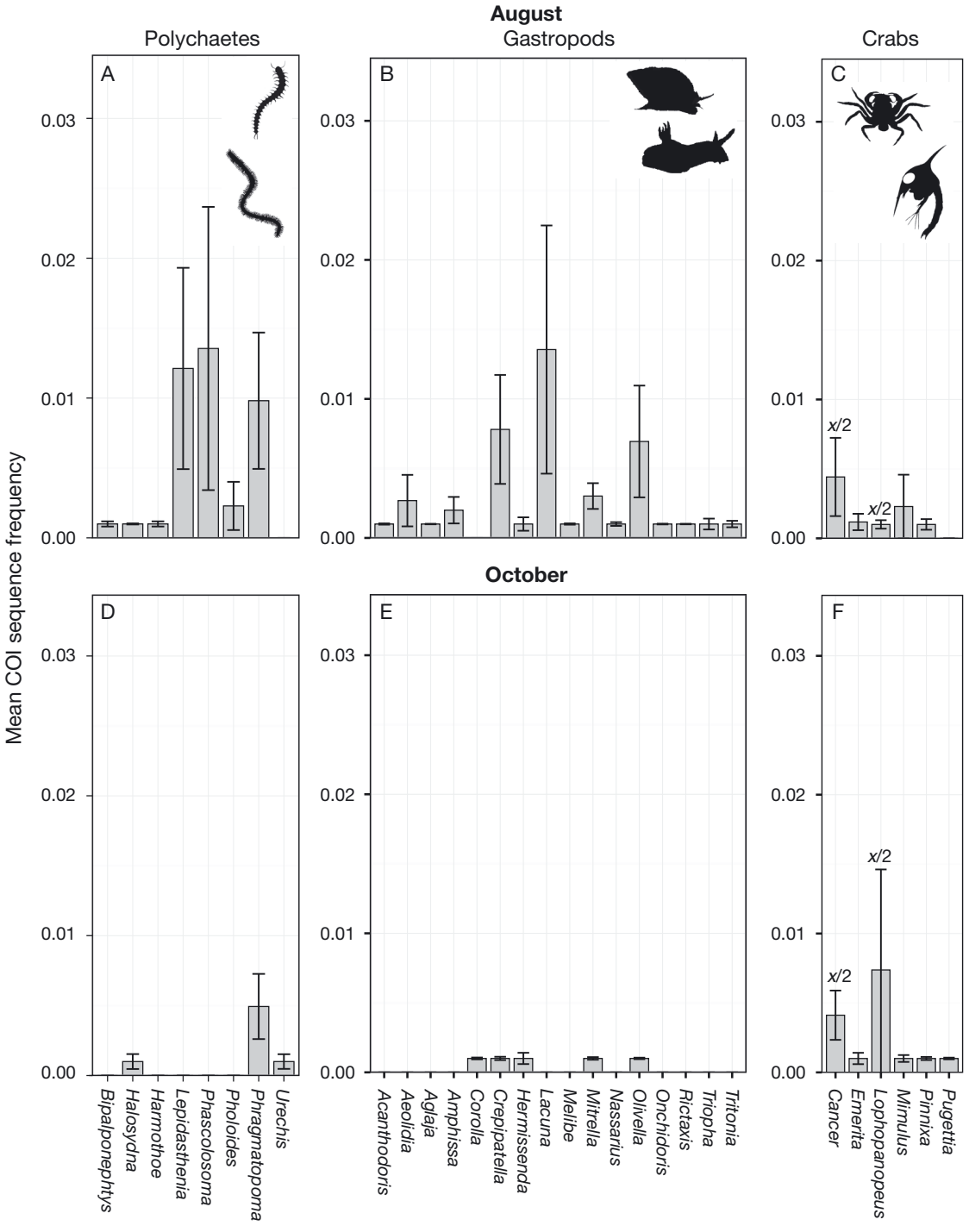

Fig. 7. Variation in mean COI sequence frequencies for (A,D) polychaetes, (B,E) gastropods and (C,F) crabs between August (A–C) and October (D–F) sampling periods. Mean COI sequence frequencies (*y*-axes; % total sample library size) are shown for various genera (*x*-axes). For the crabs *Cancer* and *Lophopanopeus*, *x*/2 indicates scaling of *y*-axis values by one-half to facilitate visualization; *y*-axis values >0 but <0.001 were plotted as 0.001 improve presence/absence visualization. Error bars: SE

Discrepancies among data sets

As previously noted, discrepancies existed among the COI, 28S and morphological data sets, due to biases inherent in each method (Harvey et al. 2017). Consequently, different data sets did not always detect the same taxa (Table 1). For example, echinoderm 28S data identified 3 species, but none corre-

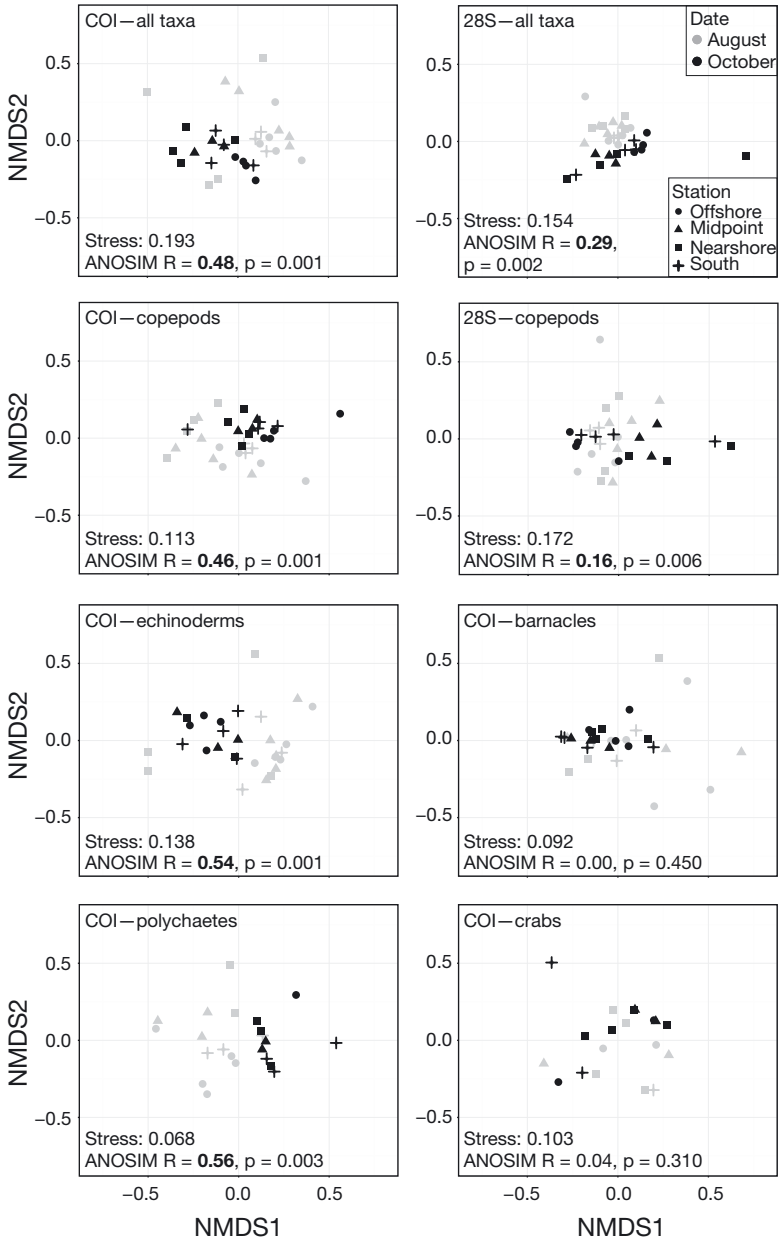

Fig. 8. Non-metric multidimensional scaling (NMDS) ordination of Bray-Curtis dissimilarity indices for zooplankton high-throughput DNA sequencing (HTS) data. Data sets (upper left-hand corners), NMDS stress (Kruskal), and corresponding ANOSIM values for each plot are indicated (lower left-hand corners). Significant ANOSIM R-values ($p < 0.01$) are in **bold**. Samples are differentiated by sampling period and station. Only stations sampled during both periods were included (i.e. Nearshore, Midpoint, Offshore, and South). Data sets that lacked sufficient variation between sampling periods to achieve convergent solutions by ordination were not included (e.g. echinoderm, barnacle, polychaete and crab 28S)

sponded to those identified by COI. Similarly, less than half of the copepod taxa detected by COI were also identified by 28S or the morphological analysis. Morphologically identified barnacle genera were also identified by COI, however, 28S only detected one of these (i.e. *Balanus*). COI data identified more polychaete, gastropod and crab taxa than 28S. COI also primarily identified different genera than 28S, with the exception of the polychaete *Phascolosoma*, the gastropods *Amphissa* and *Nassarius*, and the crabs *Emerita* and *Pinnixa*.

In addition to discrepancies in identification, taxonomic resolution also varied among data sets. For example, the morphological assessment identified echinoderms, but taxonomic resolution did not extend below the Phylum level. Likewise, morphological analysis did not resolve taxa within the Classes Polychaeta or Gastropoda, unlike the HTS data sets. Conversely, morphological analysis identified life stages, while HTS data did not (Harvey et al. 2017). Additionally, the morphological analysis identified 12 crab taxa, but HTS data detected only a subset of these.

Aside from taxonomic discrepancies, data sets also occasionally disagreed as to where and when organisms occurred. For example, COI and morphology only identified the copepod *Metridia* in August, but 28S detected the genus during both sampling periods. Similarly, COI and morphology identified *Balanus* and *Emerita* during both sampling periods, but 28S only detected them in August. Spatial discrepancies among data sets included *Cancer* identification by morphology but not COI at Stn South (August), and *Lophopanopeus* identification by both morphology and COI in August, but only by COI in October.

DISCUSSION

Seasonal environmental changes

A seasonal shift associated with reduced upwelling and intrusion of low-salinity waters from the California Current is typical for northern Monterey Bay, California (Broenkow & Smethie 1978, Rosenfeld et al. 1994, Ramp et al. 2005). We documented this shift with data from the M1 mooring at the mouth of the Bay

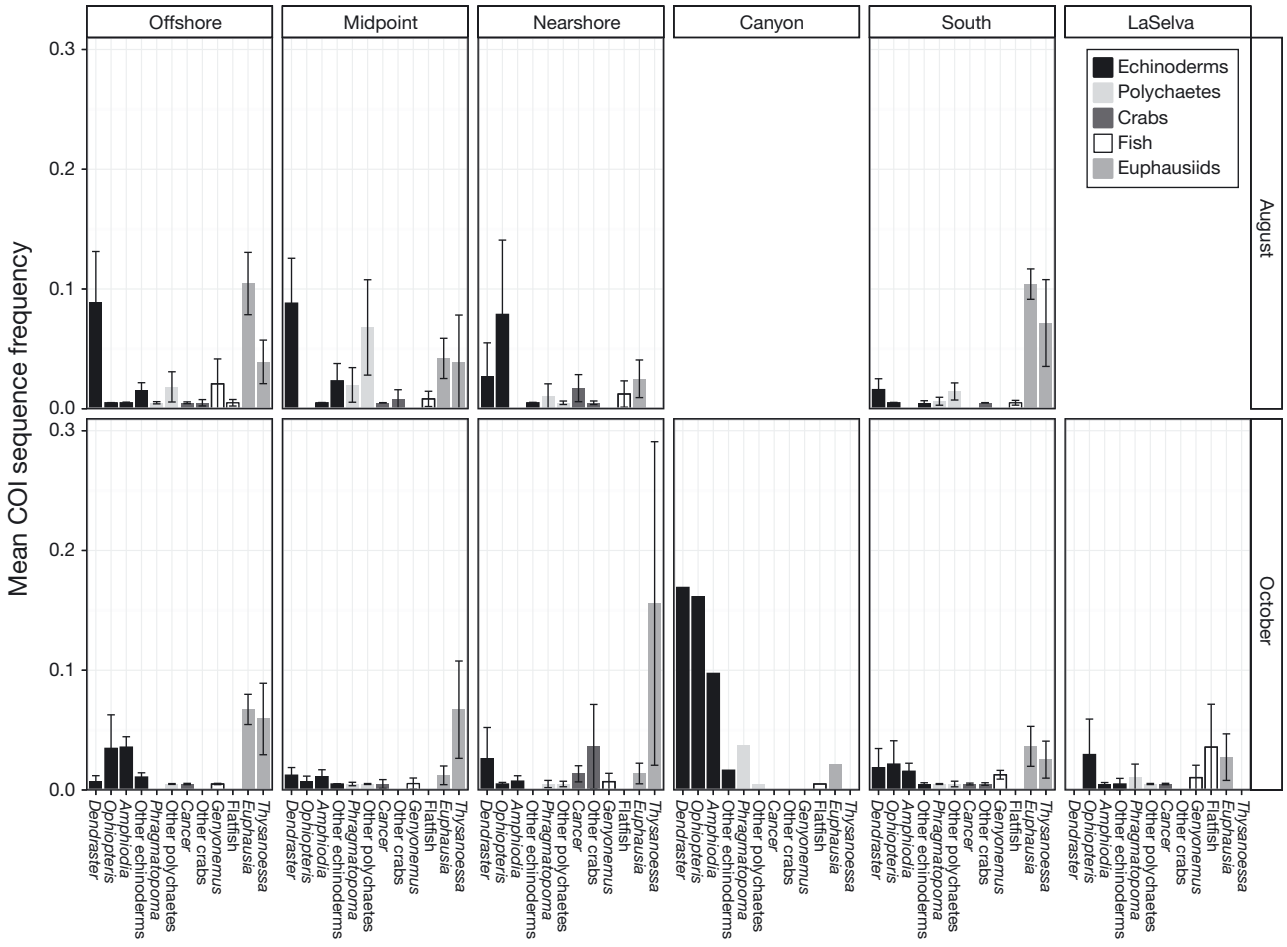

Fig. 9. Variation in mean COI sequence frequencies among stations and between sampling periods for echinoderms, polychaetes, crabs, fish and euphausiids. Mean COI sequence frequencies (*y*-axis; % total sample library size) are shown for various taxa (*x*-axis); *y*-axis values were scaled to facilitate visualization for the following taxa: *Cancer*, *Lophopanopeus*: *x*/2; *Euphausia*: *x*/4; *Thysanoessa* (*x*)100; *y*-axis values >0 but <0.005 were plotted as 0.005 to improve presence/absence visualization. Error bars: SE. Results are faceted by station (columns) and sampling period (rows). Missing facets (i.e. August: Canyon and La Selva stations) indicate no samples were collected. Results for the Canyon station in October lack error bars because this location was only sampled once

Table 3. Total zooplankton biomass by station for August and September sampling periods. (–) Missing data (i.e. samples not collected)

	Biomass (mg C m^{-3} seawater)					
	Offshore	Midpoint	Nearshore	Canyon	South	LaSelva
August						
Echinodermata	0.515	0.175	0.060	–	0.040	–
Polychaeta	0.718	1.619	0.317	–	0.298	–
Decapoda	10.362	2.320	2.410	–	0.967	–
Actinopteri	0.302	0.000	0.000	–	0.000	–
Euphausia pacifica	6.231	0.500	0.216	–	3.543	–
Thysanoessa spinifera	0.795	1.186	0.592	–	0.600	–
October						
Echinodermata	–	0.000	–	0.355	0.154	–
Polychaeta	–	0.186	–	0.411	0.142	–
Decapoda	–	7.597	–	0.430	0.441	–
Actinopteri	–	1.086	–	0.202	0.000	–
Euphausia pacifica	–	0.090	–	0.000	0.000	–
Thysanoessa spinifera	–	0.000	–	0.000	0.000	–

and from 'Dorado' AUV transects in the northern Bay. The 'Dorado' AUV provided high-resolution synoptic temperature and salinity profiles, greatly surpassing the view of environmental variation along our sampling transects possible by any other means. The morphological and molecular data documented corresponding shifts in zooplankton communities.

Zooplankton community variation

Copepod species richness escalated as biomass declined after offshore waters intruded into Monterey Bay during the fall transition period of 2013. Similar shifts are known to occur during winter conditions off the Oregon coast (Hooff & Peterson 2006). Increased species richness of copepods and other taxa typically follow intrusions of warmer offshore waters (Keister & Peterson 2003, Bi et al. 2011, Keister et al. 2011). Conversely, decreased copepod diversity and increased biomass occur during summer when cooler water driven by the California Current enters these coastal environments (Hooff & Peterson 2006). Species we observed during October (*Calocalanus tenuis*, *Rhincalanus nasutus*, *Calanus pacificus*, *Clausocalanus* spp. and *Paracalanus* sp.) are associated with warmer, southern, offshore waters (Hooff & Peterson 2006). Shifts in the lipid content (i.e. caloric value) of copepods during these seasonal transitions affect the recruitment success of salmonids and other commercial fisheries (Peterson et al. 2014).

Echinoderm biomass also increased between the sampling periods. COI sequences for *Rathbunaster* first appeared during October as *Ophiopteris* and *Amphiodia* increased in frequency, suggesting that these taxa were delivered shoreward with the intrusion of offshore waters. Northward wind stress and onshore water flow coincide with increases of larval echinoderms and peak settlement at leeward coastal sites (Miller & Emlet 1997).

Barnacle biomass and *Balanus* COI frequencies also increased between the sampling periods. Episodic transport of barnacle larvae by onshore flow mechanisms (e.g. internal waves, upwelling fronts) was previously documented for Monterey Bay and elsewhere (Pineda 1991, Roughgarden et al. 1991, Ryan et al. 2014a).

Polychaetes and gastropods exhibited a decline in COI sequence richness and overall biomass during the fall transition. Settlement of juvenile life-history stages could account, in part, for this decline. Although factors affecting invertebrate larval settlement vary (Pawlik 1992, Qian 1999), sediment-associated biofilms induce settlement for polychaetes (Sebesvari et al. 2006, Hadfield et al. 2014) and gastropods (Zhao & Qian 2002), as does the presence of benthic adults (Cahill & Koury 2016). Reduced vertical stratification (e.g. mixing) prior to October sampling could have increased benthic sampling cues in the water column.

Although crab biomass increased between sampling periods, sequences from several taxa decreased in frequency. Crab megalopae also respond to settlement cues from adults and the benthic environment (Forward et al. 2001, Simith et al. 2010). Nevertheless, behavioral mechanisms that mediate presettlement transport of crab larvae might also be responsible for the observed shifts in crab biomass (Morgan 2014).

Seasonal shifts in species richness and biomass were responsible for community-level changes, as illustrated by NMDS results. Community-level shifts in COI sequence richness primarily resulted from changes in the frequencies of copepod, echinoderm and polychaete sequences. Frequencies of echinoderm and polychaete sequences varied most, generating the greatest ANOSIM R-values (Fig. 8). Conversely, barnacles and crabs did not vary significantly. Though less discriminating at lower taxonomic levels, the 28S rRNA data also revealed significant seasonal shifts (e.g. for 'all taxa' and 'copepods', Fig. 4). Although COI and 28S sequences identified few taxa in common (due to primer or other locus-specific biases), both markers led to similar conclusions regarding a community shift between the 2 sampling periods.

Spatial distributions

The distribution and abundance of zooplankton in coastal environments are governed by many factors, including physical forces (Woodson et al. 2009, Morgan et al. 2011, Ryan et al. 2014a), behavioral mechanisms (Morgan & Fisher 2010, Morgan 2014) and life-stage variation (Peterson 1998, Abookire & Bailey 2007). Movements of surface water probably influenced the distribution of echinoderm larvae during the 2 sampling periods. For example, the pluteus larvae of *Dendraster* inhabit surface waters and are capable of limited vertical migration (Pennington & Emlet 1986, Pedrotti & Fenaux 1992). Shoreward delivery driven by northward wind stress may have been responsible for increased echinoderm biomass (Miller & Emlet 1997) and increased frequencies for *Amphiodia.* During October, COI sequences for *Amphiodia* were greatest at the Offshore and Canyon

stations, suggesting delivery by shoreward intrusion of offshore waters.

Polychaetes and crabs were differentially distributed among stations and between sampling periods. Concentrations and movements of larvae due to internal waves (Pineda 1991, Shanks 2006), subsurface layers (Ryan et al. 2010a) and upwelling shadows (Graham et al. 1992, Morgan et al. 2011) can influence larval distributions. Species-specific behavioral mechanisms also govern distributions of crab larvae, enabling nearshore retention or offshore migration (Morgan & Fisher 2010, Morgan 2014).

Distributions of larval fish are also influenced by behaviors (e.g. diurnal vertical migration; Sakuma et al. 1999) and vary seasonally with shifts in temperature (Walker et al. 1987). Movements of highly mobile spawning adults will also affect these patterns (e.g. white croaker; Ahr et al. 2015). Sole modify their locations for spawning and move progressively shoreward throughout development (Abookire & Bailey 2007). Although the adult distributions were unknown, our samples contained fish eggs that probably provided most of the COI sequences we encountered. Surface waters near spawning areas often contain buoyant fish eggs (Abookire & Bailey 2007) that are subjected to a number of physical forces. For example, the buoyancy and vertical distribution of fish eggs are affected by salinity, irrespective of temperature (Sundby & Kristiansen 2015). Decreases in salinity during October might have influenced fish egg buoyancy, thereby resulting in the reduced detection of fish COI sequences.

Euphausiid COI sequences and biomass decreased between August and October, in agreement with previous krill surveys in the Monterey Bay (Croll et al. 2005). *Euphausia pacifica* occurred at every station and *Thysanoessa spinifera* was present at most stations during both sampling periods. Nonetheless, *E. pacifica* sequences and biomass were greatest at the offshore stations. Maximum krill abundances in Monterey Bay typically occur offshore and decrease toward shore (Santora et al. 2011a,b). Conversely, *T. spinifera* sequences did not exhibit a similar trend.

Data set biases

In general, HTS can provide greater estimates of meroplankton biodiversity than morphological analysis alone (Lindeque et al. 2013, Harvey et al. 2017, Hirai et al. 2017). However, methodological biases associated with HTS estimates of biodiversity are known (Porazinska et al. 2009, Bik et al. 2012, Cowart et al. 2015). Primer sequence variation among the target organisms, PCR amplification biases and the inclusiveness of reference databases for various genes all potentially affect detection frequencies and taxonomic assignment accuracy (Harvey et al. 2017). Furthermore, false positive assignments to closely related taxa could have created discrepancies if sequence data for some taxa were not available. Indeed, it is clear that reference sequences for some taxa were not always present in our NCBI-derived reference sequence databases (Table 1). Nonetheless, morphological assessments of biodiversity are biased, as well, by the existence of morphologically cryptic taxa (particularly larval stages), variation in the taxonomic expertise of researchers and difficulty in estimating total biomass for immature life stages (e.g. copepod nauplii). These biases may complement or contradict one another. For example, COI frequencies and morphologically determined biomass increased for 2 copepods (*Calanus*, *Calocalanus*) between the sampling periods. Conversely, COI frequencies and biomass were discordant for *Paracalanus*. Although sequence frequencies generated by HTS correspond with biomass for some taxa, the relationship appears to be taxon-specific, and possibly locus-specific (for more details, see Harvey et al. 2017).

Other biases included inconsistent target detection and varying resolution among HTS and morphological data sets. For example, COI and 28S consistently detected different taxa, due perhaps to PCR primer biases, although database biases (e.g. taxonomic discrepancies among databases; Table 1) may have contributed as well (Cowart et al. 2015, Harvey et al. 2017, Morard et al. 2018). Variation in taxonomic resolution was also due in part to limits of our taxonomic expertise. For example, morphology identified the presence of unspecified fish eggs, whereas COI revealed the presence of 5 teleost species. Conversely, morphological identifications exceeded HTS with respect to numbers of crab taxa. Limited availability of target DNA, PCR primer biases or subsampling of net tows probably contributed to decreased HTS resolution of crab taxa (Cowart et al. 2015, Harvey et al. 2017). Similarly, disagreements among data sets regarding when and where taxa occurred could be attributed to various biases present at the sampling, sample processing or HTS data analysis stages.

CONCLUSIONS

An environmental shift between August and October sampling periods contributed to variation in zoo-

plankton assemblages in northern Monterey Bay. Influx of warmer, southern waters from offshore transported diverse copepod species into the Bay. Echinoderm and barnacle larvae were similarly transported shoreward by intrusion of offshore waters. Conversely, polychaete and gastropod larvae decreased in richness and abundance following this shift. Seasonal changes in the distribution of various taxa also existed among sampling stations in Monterey Bay.

The morphological and HTS methods we used to assess zooplankton diversity exhibited taxon- and locus-specific biases. Pilot studies comparing HTS results to morphologically based estimates of biomass are needed before HTS estimates of relative abundance can be reliably inferred for any given taxon. Ultimately, the HTS and morphological data used in this study complemented one another to characterize shifts in zooplankton communities following environmental changes associated with the fall transitional period in Monterey Bay. If judiciously interpreted and supported by morphological assessments, HTS represents a welcome complement to traditional microscopy for assessing variation in zooplankton assemblages.

AUV-based environmental sampling and HTS taxonomic methods expanded the results of the present study well beyond what was previously possible with traditional shipboard sampling and morphological taxonomy alone. The novel contribution of autonomously collected synoptic environmental data by an AUV allowed characterization of an environmental shift and associated influx of offshore water with previously unattainable spatial and temporal resolution. Likewise, HTS results contributed higher taxonomic resolution for some groups than was possible for the morphological analysis. Overall, as AUV and HTS methods become increasingly common, we expect that a clearer understanding of how physical mechanisms specifically affect different groups of planktonic organisms in coastal oceans will continue to emerge.

Acknowledgements. Research supported by the David and Lucile Packard Foundation was conducted at MBARI (project #901026). We dedicate this paper to our late coauthor and friend, William T. Peterson, whose expertise and participation directed our field studies. Bill's noteworthy accomplishments as a zooplankton ecologist, and his work furthering ecosystem-based management of fisheries stand as examples of academic excellence. He was an inspiration to all of us and will be dearly missed.

LITERATURE CITED

Abookire AA, Bailey KM (2007) The distribution of life cycle stages of two deep-water pleuronectids, Dover sole (*Microstomus pacificus*) and rex sole (*Glyptocephalus zachirus*), at the northern extent of their range in the Gulf of Alaska. J Sea Res 57:198–208

Ahr B, Farris M, Lowe CG (2015) Habitat selection and utilization of white croaker (*Genyonemus lineatus*) in the Los Angeles and Long Beach harbors and the development of predictive habitat use models. Mar Environ Res 108:1–13

Altschul SF, Gish W, Miller W, Myers EW, Lipman DJ (1990) Basic local alignment search tool. J Mol Biol 215:403–410

Baek SY, Jang KH, Choi EH, Ryu SH and others (2016) DNA barcoding of metazoan zooplankton copepods from South Korea. PLOS ONE 11:e0157307

Bakun A (1973) Coastal upwelling indices, west coast of North America, 1946–71. NOAA Tech Rep NMFS SSRF-671. National Marine Fisheries Service, Seattle, WA

Barber RT, Smith RL (1981) Coastal upwelling ecosystems. In: Longhurst AR (ed) Analysis of marine ecosystems. Academic Press, London, p 31–68

Beals EW (1984) Bray-Curtis ordination: an effective strategy for analysis of multivariate ecological data. Adv Ecol Res 14:1–55

Bi H, Peterson WT, Strub PT (2011) Transport and coastal zooplankton communities in the northern California Current system. Geophys Res Lett 38:L12607

Bik HM, Porazinska DL, Creer S, Caporaso JG and others (2012) Sequencing our way towards understanding global eukaryotic biodiversity. Trends Ecol Evol 27: 233–243

Breaker LC, Broenkow WW (1994) The circulation of Monterey Bay and related processes. Oceanogr Mar Biol Annu Rev 32:1–64

Broenkow WW, Smethie WM Jr (1978) Surface circulation and replacement of water in Monterey Bay. Estuar Coast Mar Sci 6:583–603

Bucklin A, Ortman BD, Jennings RM, Nigro LM and others (2010) A 'Rosetta Stone' for metazoan zooplankton: DNA barcode analysis of species diversity of the Sargasso Sea (Northwest Atlantic Ocean). Deep Sea Res II 57: 2234–2247

Bucklin A, Lindeque PK, Rodriguez-Ezpeleta N, Albaina A, Lehtiniemi M (2016) Metabarcoding of marine zooplankton: prospects, progress and pitfalls. J Plankton Res 38: 393–400

Cahill AE, Koury SA (2016) Larval settlement and metamorphosis in a marine gastropod in response to multiple conspecific cues. PeerJ 4:e2295

Caporaso JG, Kuczynski J, Stombaugh J, Bittinger K and others (2010) QIIME allows analysis of high-throughput community sequencing data. Nat Methods 7:335–336

Chavez FP, Messié M (2009) A comparison of eastern boundary upwelling ecosystems. Prog Oceanogr 83: 80–96

Cheng F, Wang M, Li C, Sun S (2014) Zooplankton community analysis in the Changjiang River estuary by single-gene-targeted metagenomics. Chin J Oceanology Limnol 32:858–870

Clarke KR (1993) Non-parametric multivariate analyses of changes in community structure. Aust J Ecol 18:117–143

Collins CA, Pennington JT, Castro CG, Rago TA, Chavez FP (2003) The California Current system off Monterey, California: physical and biological coupling. Deep Sea Res II 50:2389–2404

Cowart DA, Pinheiro M, Mouchel O, Maguer M and others (2015) Metabarcoding is powerful yet still blind: a comparative analysis of morphological and molecular surveys of seagrass communities. PLOS ONE 10:e0117562

Croll DA, Marinovic B, Benson S, Chavez FP and others (2005) From wind to whales: trophic links in a coastal upwelling system. Mar Ecol Prog Ser 289:117–130

de Vargas C, Audic S, Henry N, Decelle J and others (2015) Eukaryotic plankton diversity in the sunlit ocean. Science 348:1261605

Deagle BE, Clarke LJ, Kitchener JA, Polanowski AM, Davidson AT (2018) Genetic monitoring of open ocean biodiversity: an evaluation of DNA metabarcoding for processing continuous plankton recorder samples. Mol Ecol Resour 18:391–406

Edgar RC (2010) Search and clustering orders of magnitude faster than BLAST. Bioinformatics 26:2460–2461

Faith DP, Minchin PR, Belbin L (1987) Compositional dissimilarity as a robust measure of ecological distance. Vegetatio 69:57–68

Fleminger A (1967) Distributional atlas of calanoid copepods in the California Current region, part II. CCOFI Atlas 7: 1–215

Forward RB, Tankersley RA, Rittschof D (2001) Cues for metamorphosis of brachyuran crabs: an overview. Am Zool 41:1108–1122

Frost B, Fleminger A (1968) A revision of the genus *Clausocalanus* (Copepoda: Calanoida) with remarks on distributional patterns in diagnostic characteristics. Bull Scripps Inst Oceanogr 12:1–235

Gardner GA, Szabo J (1982) British Columbia pelagic marine Copepoda: an identification manual and annotated bibliography, Vol 62. Department of Fisheries and Oceans, Ottawa

Geller J, Meyer C, Parker M, Hawk H (2013) Redesign of PCR primers for mitochondrial cytochrome c oxidase subunit I for marine invertebrates and application in all-taxa biotic surveys. Mol Ecol Resour 13:851–861

Graham WM (1993) Spatiotemporal scale assessment of an 'upwelling shadow' in northern Monterey Bay, California. Estuaries 16:83–91

Graham WM, Largier JL (1997) Upwelling shadows as nearshore retention sites: the example of northern Monterey Bay. Cont Shelf Res 17:509–532

Graham WM, Field JG, Potts DC (1992) Persistent upwelling shadows and their influence on zooplankton distributions. Mar Biol 114:561–570

Hadfield M, Nedved BT, Wilbur S, Koehl MAR (2014) Biofilm cue for larval settlement in *Hydroides elegans* (Polychaeta): Is contact necessary? Mar Biol 161:2577–2587

Harvey JBJ, Ryan JP, Marin R, Preston CM and others (2012) Robotic sampling, in situ monitoring and molecular detection of marine zooplankton. J Exp Mar Biol Ecol 413:60–70

Harvey JBJ, Johnson SB, Fisher JL, Peterson WT, Vrijenhoek RC (2017) Comparison of morphological and next generation DNA sequencing methods for assessing zooplankton assemblages. J Exp Mar Biol Ecol 487:113–126

Hirai J, Tsuda A (2015) Metagenetic community analysis of epipelagic planktonic copepods in the tropical and subtropical Pacific. Mar Ecol Prog Ser 534:65–78

Hirai J, Kuriyama M, Ichikawa T, Hidaka K, Tsuda A (2015a) A metagenetic approach for revealing community structure of marine planktonic copepods. Mol Ecol Resour 15: 68–80

Hirai J, Yasuike M, Fujiwara A, Nakamura Y and others (2015b) Effects of plankton net characteristics on metagenetic community analysis of metazoan zooplankton in a coastal marine ecosystem. J Exp Mar Biol Ecol 469:36–43

Hirai J, Katakura S, Kasai H, Nagai S (2017) Cryptic zooplankton diversity revealed by a metagenetic approach to monitoring metazoan communities in the coastal waters of the Okhotsk Sea, northeastern Hokkaido. Front Mar Sci 4:379

Hooff RC, Peterson WT (2006) Copepod biodiversity as an indicator of changes in ocean and climate conditions of the northern California Current ecosystem. Limnol Oceanogr 51:2607–2620

Keister JE, Peterson WT (2003) Zonal and seasonal variations in zooplankton community structure off the central Oregon coast, 1998–2000. Prog Oceanogr 57:341–361

Keister JE, Di Lorenzo E, Morgan CA, Combes V, Peterson WT (2011) Zooplankton species composition is linked to ocean transport in the northern California Current. Glob Change Biol 17:2498–2511

Leray M, Yang JY, Meyer CP, Mills SC and others (2013) A new versatile primer set targeting a short fragment of the mitochondrial COI region for metabarcoding metazoan diversity: application for characterizing coral reef fish gut contents. Front Zool 10:34

Lindeque PK, Parry HE, Harmer RA, Somerfield PJ, Atkinson A (2013) Next generation sequencing reveals the hidden diversity of zooplankton assemblages. PLOS ONE 8:e81327

Lough R (1974) Dynamics of crab larvae (Anomura, Brachyura) off the central Oregon coast, 1969–1971. PhD dissertation, Oregon State University, Corvallis, OR

Machida RJ, Hashiguchi Y, Nishida M, Nishida S (2009) Zooplankton diversity analysis through single-gene sequencing of a community sample. BMC Genomics 10:438

McCann M (2014) gb2qiime.py. www.bitbucket.org/beroe/mbari-public/src/master/molecular/gb2qiime.py

McMurdie PJ, Holmes S (2013) phyloseq: an R package for reproducible interactive analysis and graphics of microbiome census data. PLOS ONE 8:e61217

Miller BA, Emlet RB (1997) Influence of nearshore hydrodynamics on larval abundance and settlement of sea urchins *Strongylocentrotus franciscanus* and *S. purpuratus* in the Oregon upwelling zone. Mar Ecol Prog Ser 148: 83–94

Minchin PR (1987) An evaluation of the relative robustness of techniques for ecological ordination. Vegetatio 69: 89–107

Morard R, Garet-Delmas MJ, Mahe F, Romac S and others (2018) Surface ocean metabarcoding confirms limited diversity in planktonic foraminifera but reveals unknown hyper-abundant lineages. Sci Rep 8:2539

Morgan SG (2014) Behaviorally mediated larval transport in upwelling systems. Adv Oceanogr 2014:364214

Morgan SG, Fisher JL (2010) Larval behavior regulates nearshore retention and offshore migration in an upwelling shadow and along the open coast. Mar Ecol Prog Ser 404:109–126

Morgan SG, Fisher JL, Largier JL (2011) Larval retention, entrainment, and accumulation in the lee of a small headland: recruitment hot spots along windy coasts. Limnol Oceanogr 56:161–178

Park CH, Kim KM, Elvebakk A, Kim O and others (2015) Algal and fungal diversity in Antarctic lichens. J Eukaryot Microbiol 62:196–205

Pawlik JR (1992) Chemical ecology of the settlement of benthic marine invertebrates. Oceanogr Mar Biol Annu Rev 30:273–335

Pearman JK, El-Sherbiny MM, Lanzén A, Al-Aidaroos A, Irigoien X (2014) Zooplankton diversity across three Red Sea reefs using pyrosequencing. Front Mar Sci 1:27

Pedrotti ML, Fenaux L (1992) Dispersal of echinoderm larvae in a geographical area marked by upwelling

(Ligurian Sea, NW Mediterranean). Mar Ecol Prog Ser 86:217–227

Pennington JT, Chavez FP (2000) Seasonal fluctuations of temperature, salinity, nitrate, chlorophyll and primary production at station H3/M1 over 1989–1996 in Monterey Bay, California. Deep Sea Res II 47:947–973

Pennington JT, Emlet RB (1986) Ontogenetic and diel vertical migration of a planktonic echinoid larva, *Dendraster excentricus* (Eschscholtz): occurrence, causes, and probable consequences. J Exp Mar Biol Ecol 104:69–95

Peterson WT (1998) Life cycle strategies of copepods in coastal upwelling zones. J Mar Syst 15:313–326

Peterson WT, Fisher JL, Peterson JO, Morgan CA and others (2014) Applied fisheries oceanography: ecosystem indicators of ocean conditions inform fisheries management in the California Current. Oceanography (Wash DC) 27: 80–89

Pineda J (1991) Predictable upwelling and the shoreward transport of planktonic larvae by internal tidal bores. Science 253:548–551

Porazinska DL, Giblin-Davis RM, Faller L, Farmerie W and others (2009) Evaluating high-throughput sequencing as a method for metagenomic analysis of nematode diversity. Mol Ecol Resour 9:1439–1450

Qian PY (1999) Larval settlement of polychaetes. Hydrobiologia 402:239–253

R Core Team (2016) R: a language and environment for statistical computing. R Foundation for Statistical Computing, Vienna

Ramp SR, Paduan JD, Shulman I, Kindle J and others (2005) Observations of upwelling and relaxation events in the northern Monterey Bay during August 2000. J Geophys Res Oceans 110:C07013

Rosenfeld LK, Schwing FB, Garfield N, Tracy DE (1994) Bifurcated flow from an upwelling center: a cold water source for Monterey Bay. Cont Shelf Res 14:931–964

Roughgarden J, Pennington JT, Stoner D, Alexander S, Miller K (1991) Collisions of upwelling fronts with the intertidal zone — the cause of recruitment pulses in barnacle populations of Central California. Acta Oecol 12: 35–51

Royston P (1982) Algorithm AS 181: the W test for normality. Appl Stat 31:176–180

RStudio Team (2016) RStudio: integrated development for R. RStudio, Boston, MA

Ryan JP, Gower JFR, King SA, Bissett WP and others (2008) A coastal ocean extreme bloom incubator. Geophys Res Lett 35:L12602

Ryan JP, Fischer AM, Kudela RM, Gower JFR and others (2009) Influences of upwelling and downwelling winds on red tide bloom dynamics in Monterey Bay, California. Cont Shelf Res 29:785–795

Ryan JP, Johnson SB, Sherman A, Rajan K and others (2010a) Mobile autonomous process sampling within coastal ocean observing systems. Limnol Oceanogr Methods 8:394–402

Ryan JP, McManus MA, Sullivan JM (2010b) Interacting physical, chemical and biological forcing of phytoplankton thin-layer variability in Monterey Bay, California. Cont Shelf Res 30:7–16

Ryan JP, Harvey JBJ, Zhang Y, Woodson CB (2014a) Distributions of invertebrate larvae and phytoplankton in a coastal upwelling system retention zone and peripheral front. J Exp Mar Biol Ecol 459:51–60

Ryan JP, McManus MA, Kudela RM, Lara Artigas M and others (2014b) Boundary influences on HAB phytoplankton ecology in a stratification-enhanced upwelling shadow. Deep Sea Res II 101:63–79

Ryther JH (1969) Photosynthesis and fish production in the sea. Science 166:72–76

Sakuma KM, Ralston S, Roberts DA (1999) Diel vertical distribution of postflexion larval *Citharichthys* spp. and *Sebastes* spp. off central California. Fish Oceanogr 8: 68–76

Santora JA, Ralston S, Sydeman WJ (2011a) Spatial organization of krill and seabirds in the central California Current. ICES J Mar Sci 68:1391–1402

Santora JA, Sydeman WJ, Schroeder ID, Wells BK, Field JC (2011b) Mesoscale structure and oceanographic determinants of krill hotspots in the California Current: implications for trophic transfer and conservation. Prog Oceanogr 91:397–409

Sebesvari Z, Esser F, Harder T (2006) Sediment-associated cues for larval settlement of the infaunal spionid polychaetes *Polydora cornuta* and *Streblospio benedicti*. J Exp Mar Biol Ecol 337:109–120

Shanks AL (2001) An identification guide to the larval marine invertebrates of the Pacific Northwest. Oregon State University Press, Corvallis, OR

Shanks AL (2006) Mechanisms of cross-shelf transport of crab megalopae inferred from a time series of daily abundance. Mar Biol 148:1383–1398

Simith DJB, Diele K, Abrunhosa FA (2010) Influence of natural settlement cues on the metamorphosis of fiddler crab megalopae, *Uca vocator* (Decapoda: Ocypodidae). An Acad Bras Cienc 82:313–321

Sundby S, Kristiansen T (2015) The principles of buoyancy in marine fish eggs and their vertical distributions across the world oceans. PLOS ONE 10:e0138821

Tang CQ, Leasi F, Obertegger U, Kieneke A and others (2012) The widely used small subunit 18S rDNA molecule greatly underestimates true diversity in biodiversity surveys of the meiofauna. Proc Natl Acad Sci USA 109: 16208–16212

Walker HJ, Watson W, Barnett AM (1987) Seasonal occurrence of larval fishes in the nearshore Southern California Bight off San Onofre, California. Estuar Coast Shelf Sci 25:91–109

Woodson CB, Washburn L, Barth JA, Hoover DJ and others (2009) Northern Monterey Bay upwelling shadow front: observations of a coastally and surface-trapped buoyant plume. J Geophys Res Oceans 114:C12013

Yang J, Zhang X, Xie Y, Song C and others (2017) Zooplankton community profiling in a eutrophic freshwater ecosystem-lake Tai Basin by DNA metabarcoding. Sci Rep 7:1773

Zaiko A, Martinez JL, Schmidt-Petersen J, Ribicic D and others (2015) Metabarcoding approach for the ballast water surveillance — An advantageous solution or an awkward challenge? Mar Pollut Bull 92:25–34

Zhang Y, Ryan JP, Bellingham JG, Harvey JBJ, McEwen RS (2012) Autonomous detection and sampling of water types and fronts in a coastal upwelling system by an autonomous underwater vehicle. Limnol Oceanogr Methods 10:934–951

Zhang Y, Bellingham JG, Ryan JP, Godin MA (2015) Evolution of a physical and biological front from upwelling to relaxation. Cont Shelf Res 108:55–64

Zhao B, Qian PY (2002) Larval settlement and metamorphosis in the slipper limpet *Crepidula onyx* (Sowerby) in response to conspecific cues and the cues from biofilm. J Exp Mar Biol Ecol 269:39–51

Appendix. Two-way crossed ANOSIM. **Bold**: significant

	Period		Station	
	Global R	p-value	Global R	p-value
All taxa: COI	0.48	**0.001**	0.23	**0.004**
All taxa: 28S	0.29	**0.002**	0.02	0.39
Copepods: COI	0.46	**0.001**	0.26	**0.005**
Copepods: 28S	0.16	**0.006**	0.03	0.31
Echinoderms: COI	0.54	**0.001**	0.09	0.12
Barnacles: COI	0	0.45	0.05	0.75
Polychaetes: COI	0.56	**0.003**	0.27	**0.002**
Crabs: COI	0.04	0.31	0.08	0.29

Editorial responsibility: Marsh Youngbluth, Fort Pierce, Florida, USA

Submitted: December 21, 2017; Accepted: August 27, 2018
Proofs received from author(s): September 26, 2018